

Marcel Istrate

Mircea Gușă

Dragoș Machidon

# High Voltage Engineering

## Contents:

<b>I. High Voltage Generation</b>	1
I.1. HVAC Generators	1
I.1.1. Single-unit testing transformers	2
I.1.2. Cascaded transformers	5
I.1.3. Series resonant circuits	7
I.2. HVDC Generators	9
I.2.1. Half- and Full-Wave Rectifier Circuits	9
I.2.2. Voltage – Doubler Circuits	11
I.3. Impulse Voltages	12
I.3.1. Single-stage generator circuits	14
I.3.2. Multistage impulse generators	15
<b>II. Temporary Overvoltages in Power Grids</b>	18
II.1. Power transmission grids equivalents schemes	18
II.1.1. Sources	19
II.1.2. Transformers and autotransformers	19
II.1.3. Electrical lines	21
II.2. Temporary overvoltage due to capacitive effect	22
II.3. Temporary overvoltage due to unbalanced shortcircuits	26
II.4. Temporary overvoltage due to unbalanced faults	29
<b>III. Lightning Overvoltages</b>	33
III.1. Lightning discharge and lightning parameters	33
III.1.1. Lightning discharge	33
III.1.2. Lightning parameters	36
III.2. Protection of electrical installations against direct lightning strokes	38
III.2.1. Laboratory models method	39
III.2.2. Rolling sphere method	42
III.3. Lightning overvoltages on overhead power transmission lines	47
III.3.1. Computing relation of the specific number of outages	48

III.3.2.	The behavior of power lines without ground wires at direct lightning strokes	50
III.3.3.	The behavior of power lines with ground wires at direct lightning strokes	52
III.3.4.	The total specific number of disconnections	54
III.4.	Lightning overvoltages in power stations	55
<b>IV.</b>	<b>Power Equipments Insulation Coordination</b>	<b>64</b>
	<i>References</i>	<i>67</i>

# **I. High Voltage Generation**

In the field of electrical engineering and applied physics, high voltages (dc, ac, and impulse) are required for several applications. To name just a few examples:

- ✓ Electron microscopes and x-ray units require high dc voltages on the order of 100 kV or more.
- ✓ Electrostatic precipitators, particle accelerators, and so on, require high dc voltages of several kilovolts and megavolts .
- ✓ Testing the insulation of power apparatus requires high ac voltages of up to millions of volts, depending on their normal operating' voltages.
- ✓ Simulation of overvoltages that occur in power systems requires high impulse voltages of very short and longer durations.

One of the main concern of high-voltage engineers is for insulation testing of various power-system components under power-frequency ac, dc, switching, and lightning impulse voltages. Normally, in high-voltage testing, the currents are limited to a small value up to about 1 A under ac or dc voltages and a few amperes under impulse voltages [1].

In today's systems for voltages up to 245 kV the tests are still limited to lightning impulses and one-minute power frequency tests. Above 300 kV, in addition to lightning impulse and the one-minute power frequency tests, tests include the use of switching impulse voltages.

Such tests are usually performed in high voltage laboratories, which are equipped with various devices that produce high voltage. A fully equipped high voltage laboratory includes high voltage ac and dc generators, circuits for high voltage lightning and switching impulse generation. Methods of generating such high voltages are discussed below.

## **I.1. HVAC Generators**

As electric power transmission with high ac voltages predominates in our transmission and distribution systems, the most common form of testing high voltage apparatus is related to high ac voltages. It is obvious then that most research work in electrical insulation systems has to be carried out with this type of voltage.

In every laboratory HVAC supplies are therefore in common use. As far as the voltage levels are concerned, these may range from about 10 kV only up to more than 3 MV today. [2]

High ac voltage can be obtain either using transformers or using resonant circuits. For generating ac test voltages of less than a few hundred kV, a single transformer can be

used. For higher voltages, a single transformer construction would entail undue insulation problems. Also, expenses, transportation and erection problem connected with large testing transformers become prohibitive. These draw-backs are avoided by cascading several transformers of relatively small size with their high-voltage windings effectively connected in series.

A fundamental design factor for all ac testing supplies is an adequate control system for a continuous regulation of the high output voltages. In general, this will be performed by a control of the primary or low voltage input of the voltage step-up systems.

### **I.1.1. Single-unit testing transformers**

The power frequency single-phase transformer is the most common form of HVAC testing apparatus. Designed for operation at the same frequency as the normal working frequency of the test objects (i.e., 60 or 50 Hz), they may also be used for higher frequencies with rated voltage, or for lower frequencies, if the voltages are reduced in accordance to the frequency, to avoid saturation of the core.

From the considerations of thermal rating, the kVA output and the fundamental design of the iron core and windings there is not a very big difference between a testing and a single-phase power transformer. The differences are related mainly to a smaller flux density within the core to avoid unnecessary high magnetization currents which would produce higher harmonics in the voltage regulator supplying the transformer, and to a very compact and well insulated high voltage winding for the rated voltage. Therefore, a single-phase testing unit may be compared with the construction of a potential transformer used for the measurement of voltage and power in power transmission systems.

The main differences between a single-phase testing transformer and a single-phase power transformer are presented below:

- shortcircuit current on the high voltage winding must be large enough in order to generate a visible failure in the tested insulation (about 1 A for dry insulation and 3 A for wet insulation), and to avoid the appearance of significant overvoltages due to intermittent burning of the breakdown or flashover electric arc of the tested insulation;
- shortcircuit voltage must be small enough in order to ensure the necessary value of the current, and to increase the voltage on the tested equipment by reducing the internal voltage drops;
- the testing voltage must be pure sinusoidal, only a maximum of 2-5% of harmonics being allowed.

For a better understanding of advanced circuits, the fundamental design of such single-unit testing transformers will be illustrated. Figure 1.a shows the well-known circuit diagram. The primary winding '2' is usually rated for low voltages of  $\leq 1$  kV, but might often be split up in two or more windings which can be switched in series or parallel (not shown here) to increase the regulation capabilities. The iron core '1' is fixed at earth potential as well as one terminal of each of the two windings. Simplified cross-sections of two possible constructions for the unit itself are given in Figures 1.1.b,c.[2]

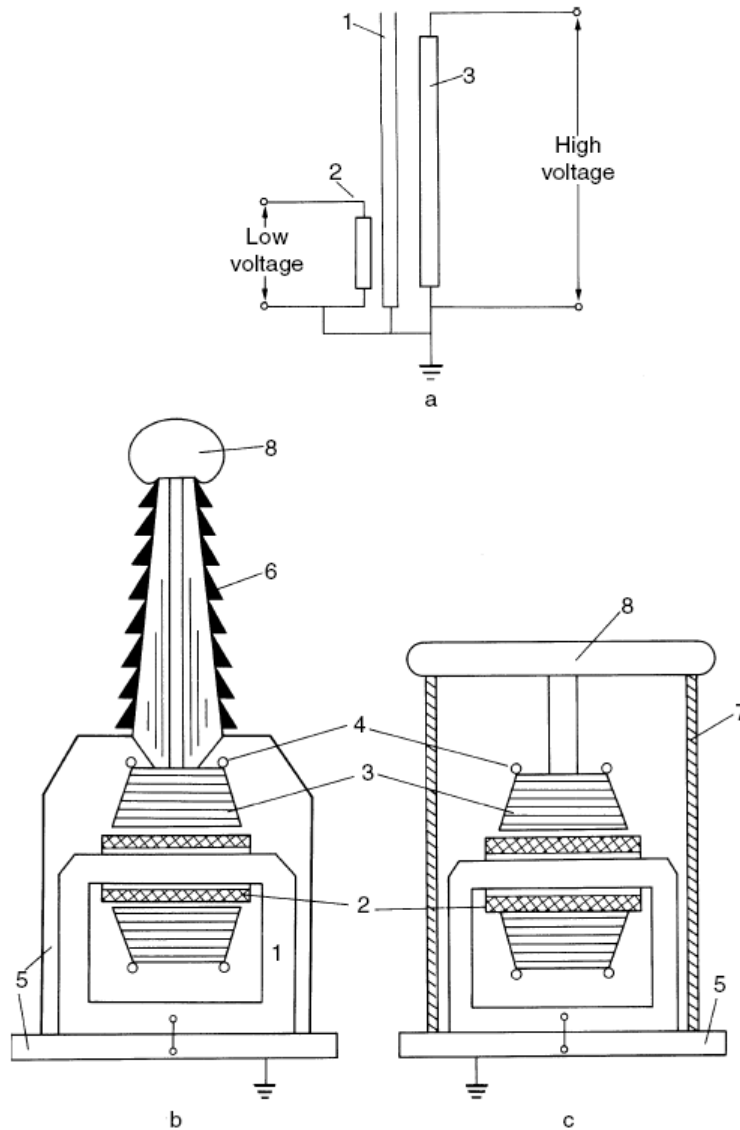


**Fig.1.1.** Single unit testing transformers. (a) Diagram. (b & c) different construction units. (1) Iron core. (2) Primary low voltage or exciting winding.(3) Secondary high voltage winding. (4) Field grading shield. (5) Grounded metal tank and base. (6) HIGH VOLTAGE bushing. (7) Insulating shell or tank. (8) HIGH VOLTAGE electrode

In both cases the layout arrangement of core and windings is basically the same. Figure 1.1.b, however, shows a grounded metal tank unit, for which an high voltage bushing '6' is necessary to bring the high voltage out of the tank '5'. Instead of a bushing, a coaxial cable could also be used if this improves the connection between testing transformer and test object. In Fig.1.1.c the active part of the transformer is housed within an isolating cylinder '7' avoiding the use of the bushing. This construction reduces the height, although the heat transfer from inside to outside is aggravated. In both cases the vessels would be filled with high-quality transformer oil, as most of the windings are oil-paper insulated.

The sectional view of the windings shows the primary winding close to the iron core and surrounded by the high voltage winding '3'. This coaxial arrangement reduces the magnetic stray flux and increases, therefore, the coupling of both windings. The shape of the cross-section view of winding no. 3 is a hint to the usual layout of this coil: the beginning (grounded end) of the high voltage winding is located at the side close to the core, and the end close to a sliced metal shield, which prevents too high field intensities at high voltage potential.

Between both ends the single turns are arranged in layers, which are carefully insulated from each other by solid materials (kraft paper sheets for instance). Adjacent layers, therefore, form coaxial capacitors of high values, and if those capacitances are equal – produced by the reduced width of the single layers with increasing diameters – the potential distribution for transient voltages can be kept constant. By this procedure, the trapezoidal shape of the cross-section is originated.

It may well be understood that the design of the high voltage winding becomes difficult if voltages of more than some 100 kV must be produced within one coil. Better constructions are available by specialized techniques, mainly by 'cascading' transformers.

The first step in this technique is to place two high voltage windings on one iron core, to join both windings in series and to connect this junction with the core. For illustration, the circuit diagram is shown in Fig.1.2. in combination with a simplified cross-section of the active part. The arrangement could still be treated as a single unit transformer, as only one core exists. The mid-point of the high voltage winding is connected to the core and to a metal tank, if such a tank is used as a vessel. The cross-section shows that the primary winding '2' is, however, placed now around the first part '3a' of the whole h.t. winding, whose inner layer, which is at half-potential of the full output voltage, is connected to the core. There are two additional windings, '4a' and '4b', rated for low voltages, which act as compensating windings.

These are placed close to the core and reduce the high leakage reactance between '3b' and the primary '2'. Often an exciting winding '5', again a winding rated for low voltages

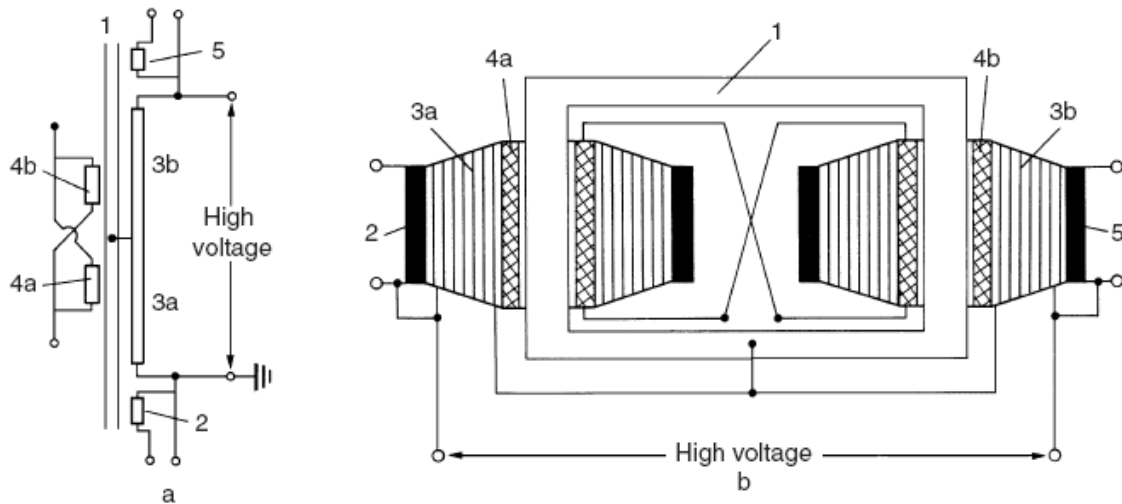


**Fig.1.2.** Single unit testing transformer with mid-point potential at core: Diagram (a) and cross-section (b). (1) Iron core. (2) Primary winding. (3a & b) High-voltage windings. (4a & b) compensating windings. (5) Exciting winding

as the primary winding, is also available. This exciting winding is introduced here as it will be needed for the cascading of transformers. Note that this winding is at the full output potential of the transformer.

Although no vessel is shown in which such a unit would be immersed, it can easily be understood that for metal tank construction (see Fig.1.1.b.) two high voltage bushings are now necessary. The tank itself must be insulated from earth for half-output voltage.

### 1.1.2 Cascaded transformers [2]

For voltages higher than about 300 to 500 kV, the cascading of transformers is a big advantage, as the weight of a whole testing set can be subdivided into single units and therefore transport and erection becomes easier.

A prerequisite to apply this technique is an exciting winding within each transformer unit as already shown in Fig.1.2. The cascading principle will be illustrated with the basic scheme shown in Fig.1.3. [2]. The low voltage supply is connected to the primary winding '1' of transformer I, designed for an high voltage output of  $V$  as are the other two transformers. The exciting winding '3' supplies the primary of the second transformer unit II; both windings are dimensioned for the same low voltage, and the potential is fixed to the high potential  $V$ . The high voltage or secondary windings '2' of both units are series connected, so that a voltage of  $2V$  is produced hereby. The addition of the stage III needs no further explanation. The tanks or vessels containing the active parts (core and windings) are indicated by dashed lines only. For a metal tank construction and the non-subdivided high voltage winding assumed in this basic scheme, the core and tank of each unit would be tapped to the low voltage terminal of each secondary winding as indi-

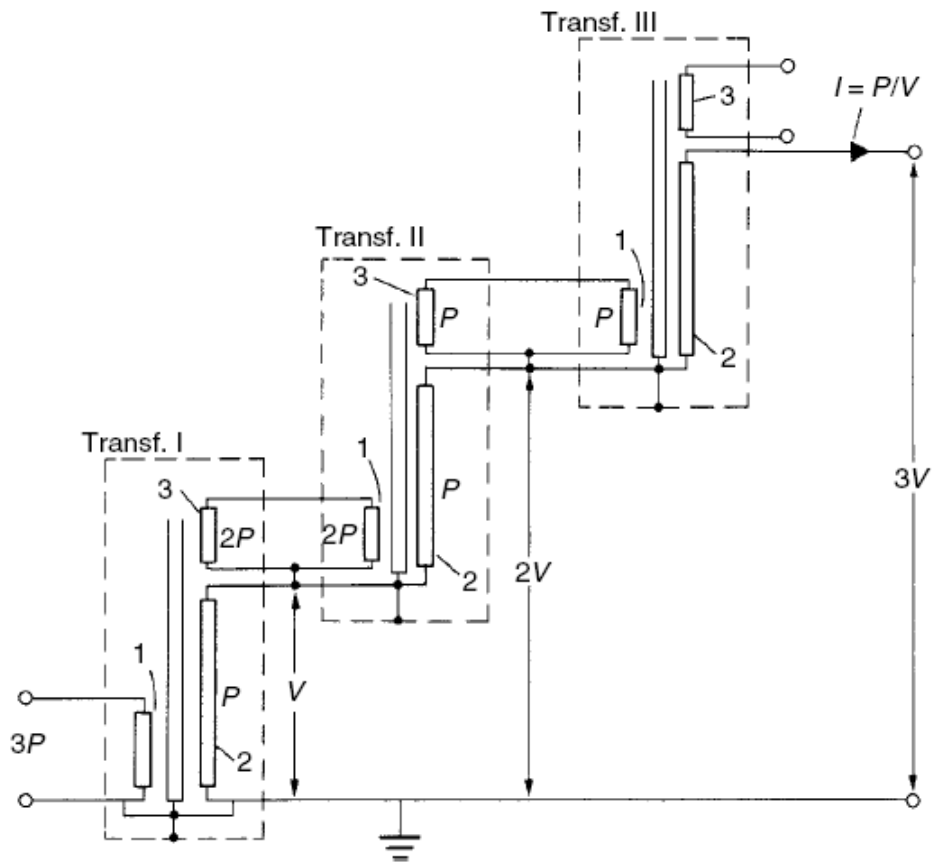


**Fig.1.3.** Basic circuit of cascaded transformers. (1) Primary windings. (2) Secondary h.t. windings. (3) Tertiary exciting windings

cated. Then the tank of transformer I can be earthed; the tanks of transformers II and III are at high potentials, namely  $V$  and  $2V$  above earth, and must be suitably insulated. Through h.t. bushings the leads from the exciting coils '3' as well as the tapings of the high voltage windings are brought up to the next transformer. If the high voltage windings of each transformer are of mid-point potential type (see Fig.1.2.), the tanks are at potentials of  $0.5V$ ,  $1.5V$  and  $2.5V$  respectively. Again, an insulating shell according to Fig.1. could avoid the h.t. bushings, rendering possible the stacking of the transformer units.

The disadvantage of transformer cascading is the heavy loading of primary windings for the lower stages. In Fig.1.3. this is indicated by the letter  $P$ , the product of current and voltage for each of the coils. For this three-stage cascade the output kVA rating would be  $3P$ , and therefore each of the h.t. windings '2' would carry a current of  $I = P/V$ . Also, only the primary winding of transformer III is loaded with  $P$ , but this power is drawn from the exciting winding of transformer II. Therefore, the primary of this second stage is loaded with  $2P$ . Finally, the full power  $3P$  must be provided by the primary of

transformer I. Thus an adequate dimensioning of the primary and exciting coils is necessary. Another important disadvantage is the fact that the short-circuit voltage of the cascade is greater as for a single-unit transformer.

As for testing of insulation, the load is primarily a capacitive one, a compensation of this capacitive load by low voltage reactors, which are in parallel to the primary windings, is possible. As these reactors must be switched in accordance to the variable load, however, one usually tries to avoid this additional expense. It might also be necessary to add tuned filters to improve the wave shape of the output voltage, that is to reduce higher harmonics.

### I.1.3 Series resonant circuits

In case of high voltage transmission cables, capsulated devices with gaseous insulation ( $\text{SF}_6$ ,  $\text{N}_2$ ), the needed power for testing such equipments becomes very large, due to the important capacitive loads of the tested objects. In order to ensure such levels of power, the dimensions of the classical testing transformers tend to become unacceptable, especially for *in-situ* testing procedures. Another problem is related to the fact that the low voltage distribution network, may not be able to provide the requested power. [3]

In this situation the technical solution that overcomes all disadvantages is represented by the series resonant circuits. The basic principle is that of the voltage resonance in a RLC circuit. A model of such series resonant circuit is represented in Figure 1.4:

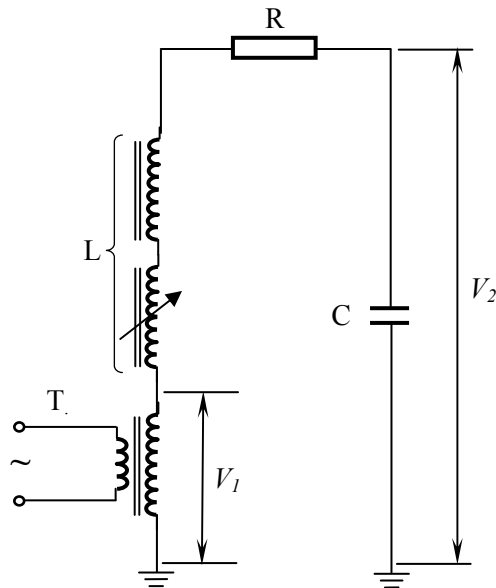


**Fig.1.4.** A basic model of a series resonant circuit

In order to obtain resonance two possibilities must be considered. Due to the various capacitance of the different objects tested, a adjustable inductance is required. Another way is to obtain resonance is by varying the supply voltage frequency, in different limits, usually 50-150 Hz.

As resonance is approached,  $V_2 \gg V_1$ , and thus it can be used a power supply transformer with a much lower rated voltage, than in case of the classical testing transformer. The efficiency of such series resonant circuits is described by a parameter named quality factor, which can be calculated with the following relation:

$$Q = \frac{V_L}{V_1} = \frac{V_C}{V_1} = \frac{V_2}{V_1} = \frac{\omega L}{R} = \frac{1}{\omega RC} \quad (1)$$

The main advantages of the series resonant circuits are:

- It is easily to obtain important values of the testing high voltage, due to the higher values of the quality factor of circuits (usually bigger than 30÷40);
- The provided voltage has an improved wave shape, not only by the elimination of unwanted resonances, but also by attenuation of harmonics already in the power supply. A realistic figure for the amplification of the fundamental voltage amplitude on resonance is between 20 and 50 times for power frequencies of 50/60 Hz. Higher harmonic voltages are divided in the series circuit with a decreasing proportion across the capacitive load. It is easily seen that harmonics in the supply become insignificant;
- The power required from the supply is lower than the kVA in the main test circuit. It represents only about 5 per cent of the main kVA with a unity power factor;
- If a failure of the test specimen occurs, no heavy power arc will develop, as only the load capacitance will be discharged. This is of great value to the cable industry where a power arc can sometimes lead to the dangerous explosion of the cable termination. It has also proved invaluable for development work as the weak part of the test object is not completely destroyed. Additionally, as the arc is self-extinguishing due to this voltage collapse, it is possible to delay the tripping of the supply circuit;[2]
- For very high voltage, cascading is also possible;
- Simple and compact test setup can be developed;
- Various degrees of sophistication are possible concerning auto-tuning devices keeping the set in tune, if supply frequency or load capacitance varies during a long-term test, or concerning auto-voltage control.

The main disadvantage is that the additional variable reactors should withstand the full-test voltage and full-current rating. Series resonance sets are usually brought into resonance by mechanical adjustment of an air gap in the iron core of the reactor. These

sets are designed and commonly used for partial discharge testing and for testing installed gas-insulated systems in the field. [1]

## I.2. HVDC Generators

Nowadays high dc voltages are used in many fields, such as pure scientific research work, HVDC transmission system equipments testing, HVAC power cables test applications, applied physics (accelerators, electron microscopy, etc.), electromedical equipment (X-rays), industrial applications (precipitation and filtering of exhaust gases in thermal power stations and the cement industry; electrostatic painting and powder coating, etc.), or communications electronics (TV, broadcasting stations).[2]

One of the main procedures used to obtain high dc voltage, consist in rectifying the high ac voltage, using different transformer - rectifying circuits which will be described further.

### I.2.1. Half- and Full-Wave Rectifier Circuits

In half-wave and full-wave rectifier circuits (e.g. Figure 1.5.), the capacitor  $C$  is gradually charged to  $V_s(\max)$ , the maximum AC secondary voltage of the  $V$  transformer during the conduction periods. During the other periods, the capacitor is discharged into the load with a time constant  $\tau = CR$ . For reasonably small ripple voltage  $\Delta V$ ,  $\tau$  should be at least 10 times the period of the AC supply. The rectifier element should have a peak inverse voltage of at least  $2V_s(\max)$ . To limit the charging current, an additional resistance is connected in series with the secondary of the transformer. [1]

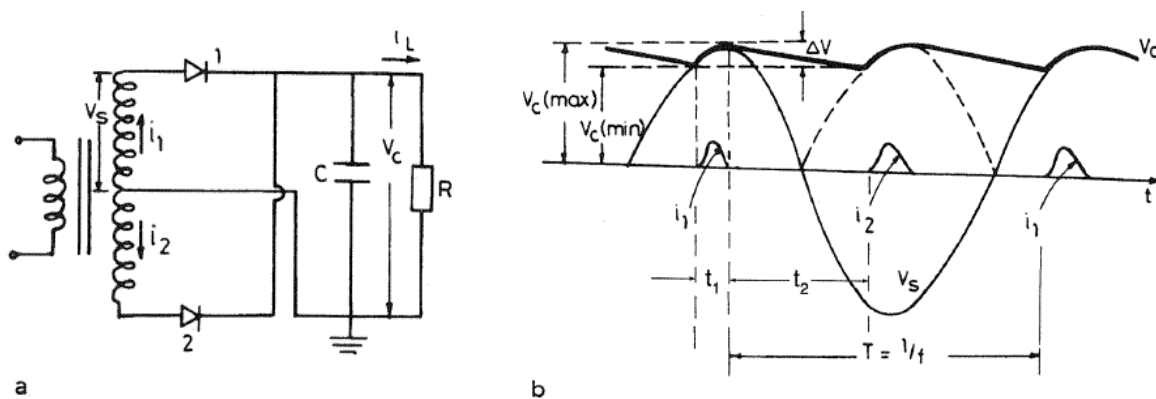


*Fig.1.5. Single-phase full wave rectifier: (a) circuit diagram, (b) steady-state voltages and currents with load R*

With half-wave rectification, and during one period  $T$  of the AC voltage, a charge  $q$  is supplied from the transformer to the capacitor within the short conduction period  $t_1$  of the rectifier element and is transferred to the load  $R$  during the long non conduction period  $t_2$ , so that:

$$q = \int_{t_1}^{t_2} i(t) dt = \int_{t_1}^{t_2} i_L(t) dt = \int_{t_1}^{t_2} \frac{V_c(t)}{R} dt = I_L T = \frac{I_L}{f} \quad (2)$$

where  $t_1 \ll t_2 \approx T = 1/f$  and  $I_L$  is the average load current.

Neglecting the voltage drops within the transformer and rectifiers during conduction,  $\Delta V$  is easily found from the charge  $q$  transferred to the load:

$$\Delta V = \frac{q}{C} = \frac{I_L}{fC} \quad (3)$$

This equation correlates the ripple voltage to the load current and the circuit parameters  $f$  and  $C$ . The product  $fC$  is an important design factor.

In full-wave rectifier circuits (Fig.1.5.), rectifiers 1 and 2 conduct during alternate half-cycles and charge the capacitor  $C$ . The HV transformer requires a center-tapped secondary with a voltage rating of  $2V_s$ .

For high voltage test circuits, a sudden voltage breakdown at the load ( $R_L \rightarrow 0$ ) must always be taken into account. Whenever possible, the rectifiers should be able to carry either the excessive currents, which can be limited by fast, electronically controlled switching devices at the transformer input, or they can be protected by an additional resistance inserted in the h.t. circuit. The last method, however, increases the internal voltage drop. Half-wave rectifier circuits have been built up to voltages in the megavolt range, in general by extending an existing high voltage testing transformer to a d.c. current supply. The largest unit has been presented by Prinz, who used a 1.2-MV cascaded transformer and 60-mA selenium-type solid state rectifiers with an overall reverse voltage of 3.4MV for the circuit. The voltage distribution of this rectifier, which is about 12m in length, is controlled by sectionalized parallel capacitor units, which are small in capacitance value in comparison with the smoothing capacitor  $C$ . The size of such circuits, however, would be unnecessarily large for pure d.c. supplies. [2]

The other disadvantage of the single-phase half-wave rectifier concerns the possible saturation of the high voltage transformer, if the amplitude of the direct current is comparable with the nominal alternating current of the transformer. The biphas half-wave (or single-phase full-wave) rectifier overcomes this disadvantage, but it does not change the fundamental efficiency, considering that two high voltage windings of the transformer are now available. With reference to the frequency  $f$  during one cycle, now each of the diodes 1 and 2 is conducting for one half-cycle with a time delay of  $T/2$ . The ripple factor is therefore halved.

## I.2.2. Voltage-Doubler Circuits

In Figure 1.6.a. [1] two half-wave rectifier circuits are connected in opposition, thus producing an unsmoothed unidirectional voltage. The source is effectively  $C_1$ ,  $C_2$ , and the transformer in series. The output voltage has a peak value of  $3V_s(\text{max})$  at no load. With the load  $R$  connected, the capacitors discharge through it with a corresponding voltage drop. This voltage doubler circuit may be earthed at any point, provided that the transformer has an adequate insulation.

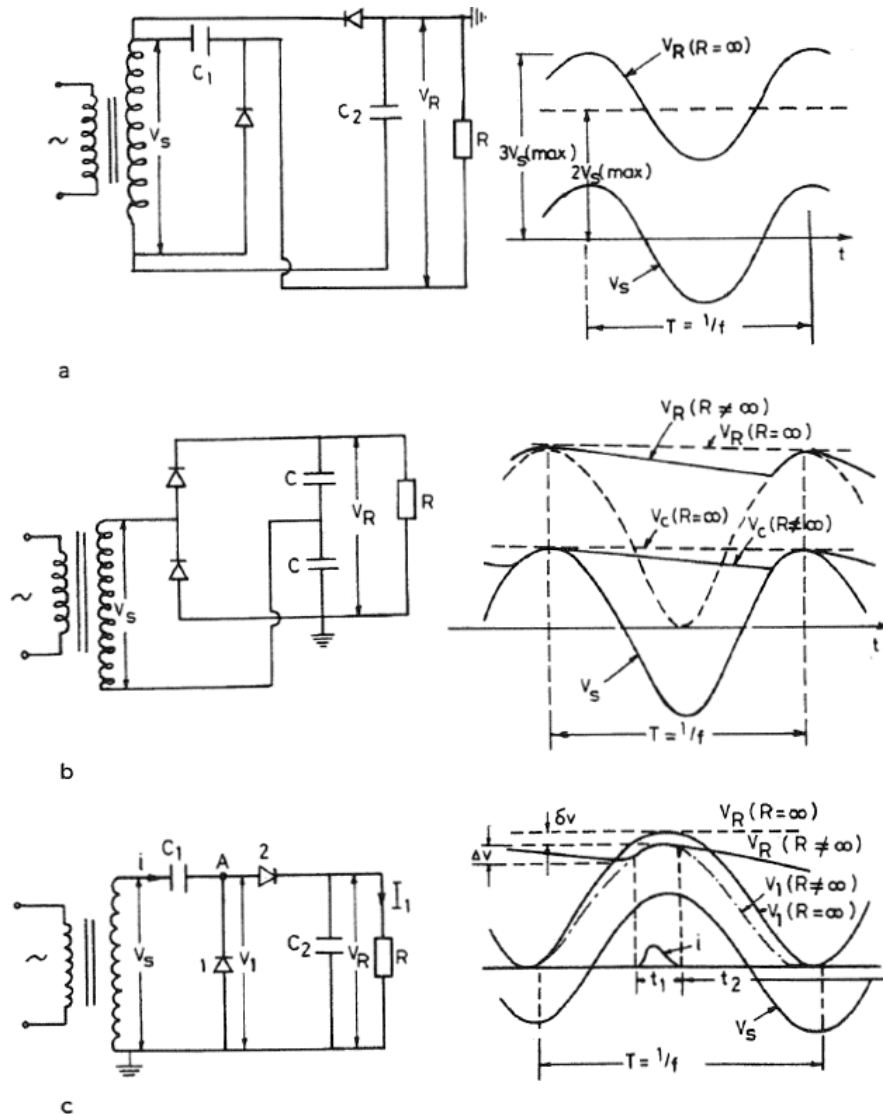


**Fig.1.6.** Connection diagrams and steady-state voltage waveforms. (a) output voltage contains a considerable ac component; (b) and (c) output voltage contains only a small ripple

In the circuit of Figure 1.6.b, each of the two capacitors is charged to only  $V_s(\text{max})$  in alternate half-cycles and the total output voltage is  $2V_s(\text{max})$  at no load, with a small ripple under load.

As the doubler of Figure 1.6.c presents the basic unit of the commonly used Cockcroft-Walton voltage-multiplier circuits, it is discussed in more detail. Rectifier 1 and capacitor  $C_1$  act as a clamp so that the voltage at node A is positive going and is clamped at  $0 V$  with a peak value of  $2V_s(\text{max})$ . Rectifier 2 conducts and charges  $C_2$  to  $2V_s(\text{max})$  when the voltage at node A is at its peak value. As the voltage at A falls below  $2V_s(\text{max})$ , rectifier 2 stops conducting as the voltage on  $C_2$  is now greater than the voltage on its anode. The capacitor  $C_2$  provides the load current until the next peak of voltage occurs at node A. Thus, the voltage at the output reaches  $2V_s(\text{max})$ . The output and input waveforms, obtained from PSpice, are shown in Figure 1.6.c (Price, 1997). It is quite clear that the doubler circuit takes a few cycles of the input for the output  $V_R$  to reach the maximum value.

### **1.3. Impulse voltages [2]**

Disturbances of electric power transmission and distribution systems are frequently caused by two kinds of transient voltages whose amplitudes may greatly exceed the peak values of the normal ac operating voltage.

The first kind are lightning overvoltages, originated by lightning strokes hitting the phase wires of overhead lines or the bus bars of outdoor substations. The amplitudes are very high, usually in the order of 1000 kV or more, as every stroke may inject lightning currents up to about 100 kA and even more into the transmission line; each stroke is then followed by travelling waves, whose amplitude is often limited by the maximum insulation strength of the overhead line. The rate of voltage rise of such a travelling wave is at its origin directly proportional to the steepness of the lightning current, which may exceed 100 kA/ $\mu\text{s}$ , and the voltage levels may simply be calculated by the current multiplied by the effective surge impedance of the line. Too high voltage levels are immediately chopped by the breakdown of the insulation and therefore travelling waves with steep wave fronts and even steeper wave tails may stress the insulation of power transformers or other high voltage equipment severely. Lightning protection systems, surge arresters and the different kinds of losses will damp and distort the travelling waves, and therefore lightning overvoltages with very different wave shapes are present within the transmission system.

The second kind is caused by switching phenomena. Their amplitudes are always related to the operating voltage and the shape is influenced by the impedances of the system as well as by the switching conditions. The rate of voltage rise is usually slower, but it is well known that the wave shape can also be very dangerous to different

insulation systems, especially to atmospheric air insulation in transmission systems with voltage levels higher than 245 kV.

Although the actual shape of both kinds of overvoltages varies strongly, it became necessary to simulate these transient voltages by relatively simple means for testing purposes. The various national and international standards define the impulse voltages as a unidirectional voltage which rises more or less rapidly to a peak value and then decays relatively slowly to zero.

In Figure 1.7. general shapes of lightning and switching impulse are presented.

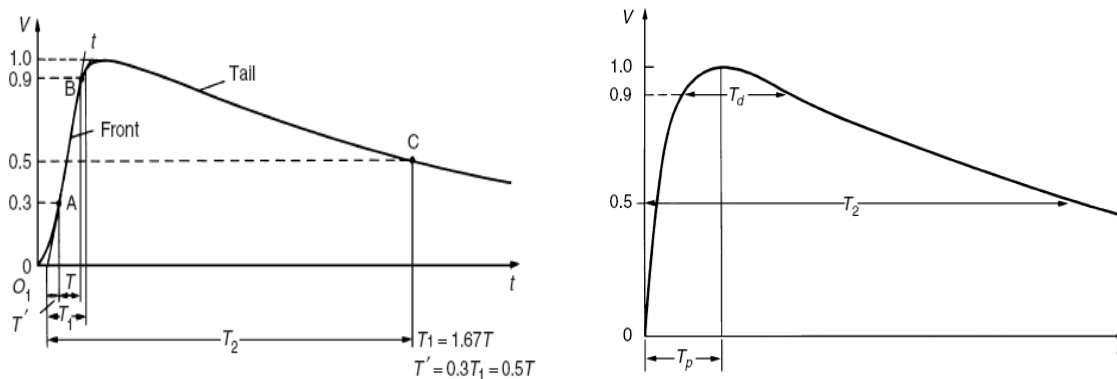


**Fig.1.7.** Standard shape of the lightning (left) and switching (right) impulse;  
 For lightning impulse:  $T_1$ : front time;  $T_2$ : time to half-value;  $O_1$ : virtual origin;  
 For switching impulse:  $T_p$ : time to peak;  $T_2$ : time to half-value;  $T_d$ : time above 90 %

Although the definitions are clearly indicated, it should be emphasized that the virtual origin,  $O_1$  is defined where the line AB cuts the time axis. The front time,  $T_1$ , again a virtual parameter, is defined as 1.67 times the interval  $T$  between the instants when the impulse is 30 per cent and 90 per cent of the peak value for full or chopped lightning impulses. For the standard lightning impulse voltage shape the front time and the time to half-value are about  $1.2 \mu\text{s}$  and  $50 \mu\text{s}$  respectively.

For the switching impulse voltage the time to half-value,  $T_2$ , is defined similarly as before, the time to peak  $T_p$  is the time interval between the *actual* origin and the instant when the voltage has reached its maximum value. This definition could be criticized, as it is difficult to establish the actual crest value with high accuracy. An additional parameter is therefore the time  $T_d$ , the time at 90 per cent of crest value. The different definitions in comparison to lightning impulses can be understood if the time scale is emphasized: the standard switching impulse has time parameters  $T_p=250 \mu\text{s}$  and  $T_2=2500 \mu\text{s}$ . Therefore is described as a 250/2500 impulse.

### I.3.1. Single-stage generator circuits

The standardized lightning impulse is generally represented by a double-exponential waveform, which may be produced in laboratory by a R-C circuit, such examples being presented in the figure below: [2]

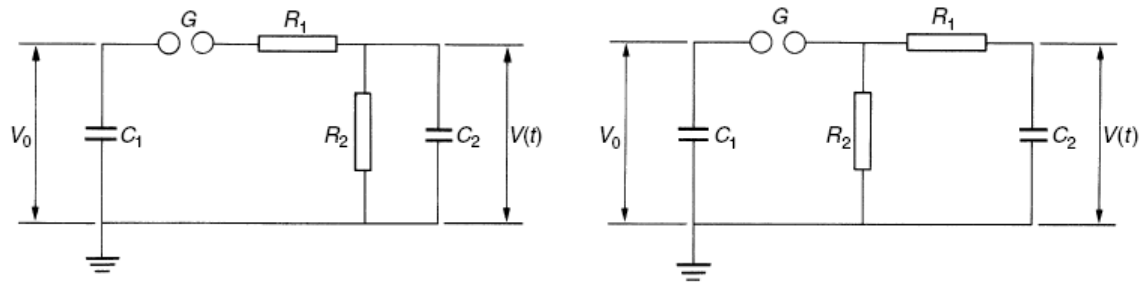


*Fig.1.8. Examples of circuits for producing impulse voltage waves*

The capacitor  $C_1$  is slowly charged from a dc source until the spark gap  $G$  breaks down. This spark gap acts as a voltage-limiting and voltage-sensitive switch, whose ignition time (time to voltage breakdown) is very short in comparison to  $T_1$ . As such single-stage generators may be used for charging voltages from some kV up to about 1MV, the sphere gaps will offer proper operating conditions. An economic limit of the charging voltage  $V_0$  is, however, a value of about 200 to 250 kV, as too large diameters of the spheres would otherwise be required to avoid excessive inhomogeneous field distributions between the spheres. The resistors  $R_1$ ,  $R_2$  and the capacitance  $C_2$  form the wave shaping network.  $R_1$  will primarily damp the circuit and control the front time  $T_1$ .  $R_2$  will discharge the capacitors and therefore essentially control the wave tail. The capacitance  $C_2$  represents the full load, i.e. the object under test as well as all other capacitive elements which are in parallel to the test object (measuring devices; additional load capacitor to avoid large variations of  $T_1/T_2$ , if the test objects are changed). No inductances are assumed so far, and are neglected in the first fundamental analysis, which is also necessary to understand multistage generators. In general this approximation is permissible, as the inductance of all circuit elements has to be kept as low as possible.[2]

The advantages of these circuits are that the wave front and wave tail are independently controlled by changing  $R_1$  and  $R_2$  separately; second, being capacitive, the test objects admittedly form a part of  $C_2$ .

The magnitudes of the different circuit elements together determine the required rapid charging of  $C_2$  to the peak value  $V_{max}$ . However, a long wave tail calls for a slow discharge. This is achieved if  $R_2$  is much larger than  $R_1$ . The smaller the time constant of the circuit, the faster is the rate by which the output voltage  $V(t)$  approaches its peak value. The peak value  $V_{max}$  cannot exceed the value determined by the distribution of the

initially available charge  $V_0$  between  $C_1$  and  $C_2$ , so the voltage efficiency is described by the following relation:[1]

$$\eta = \frac{V_{\max}}{V_0} < \frac{C_1}{C_1 + C_2} \quad (4)$$

Obviously this value is always smaller than 1, or 100 per cent.

For high efficiency,  $C_1$  should be chosen much larger than  $C_2$ . The exponential decay of the impulse voltage on the tail occurs with a time constant of about  $C_1(R_1 + R_2)$ ,  $C_1R_1$ , for the circuits presented in Fig.8 The impulse energy consumed is:

$$W = \frac{1}{2} C_1 V_0^2 \quad (5)$$

which is an important characteristic parameter of the impulse generator.

### **I.3.2. Multistage impulse generators**

Such multistage impulse generators represents the best technical solution for obtaining very high impulse voltages, using a dc source of a moderate output. Basically a bank of capacitors are charged in parallel through high ohmic resistances and then discharged in series through spark gaps, obtaining so the front and the tail of the voltage impulse waveform. [2]

To demonstrate the principle of operation, a typical circuit is presented in Figure 1.9. [2] which shows the connections of a six-stage generator. The dc voltage charges the equal stage capacitors  $C_1'$  in parallel through the high value charging resistors  $R_1'$  as well as through the discharge (and also charging) resistances  $R_2'$ , which are much smaller than the resistors  $R_1'$ . At the end of the relatively long charging period (typically several seconds up to 1 minute), the points A, B, . . . ,F will be at the potential of the dc source, e.g.  $-V$  with respect to earth, and the points G,H, . . . , N will remain at the earth potential, as the voltage drop during charging across the resistors  $R_2'$  is negligible. The discharge or firing of the generator is initiated by the breakdown of the lowest gap  $G_1$  which is followed by a nearly simultaneous breakdown of all the remaining gaps. According to the traditional theory, which does not take into account the stray capacitances indicated by the dotted lines, this rapid breakdown would be caused by high overvoltages across the second and further gaps: when the first gap fires, the potential at point A changes rapidly from  $-V$  to zero, and thus the point H increases its potential to  $+V$ . As the point B still would remain at the charging potential,  $-V$ , thus a voltage of  $2V$  would appear across  $G_2$ . This high overvoltage would therefore cause this gap to break down and the potential at

point I would rise to  $+2V$ , creating a potential difference of  $3V$  across gap  $G_3$ , if again the potential at point C would remain at the charging potential.

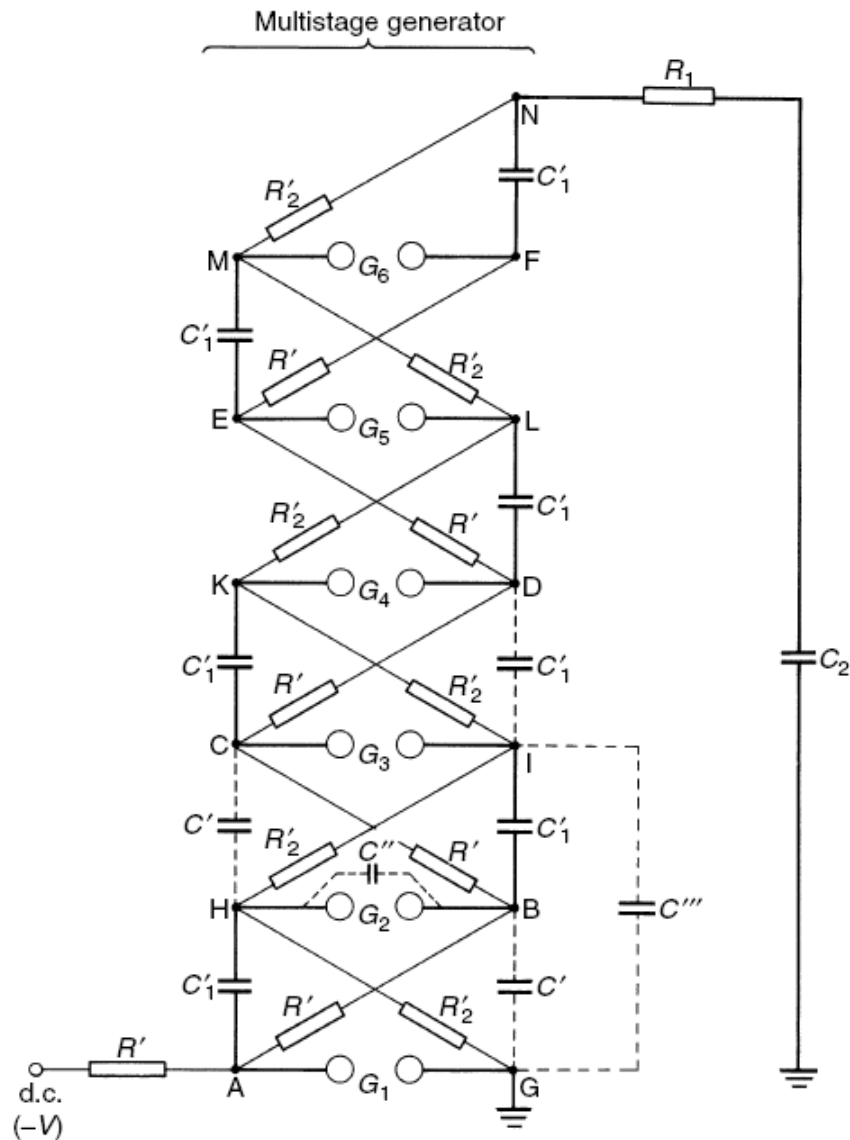


**Fig.1.9.** Basic circuit of a six-stage Marx generator

In practice for a consistent operation it is necessary to set the distance for the first gap  $G_1$  only slightly below the second and further gaps for earliest breakdown. It is also necessary to have the axes of the gaps in one vertical plane so that the ultraviolet illumination from the spark in the first gap irradiates the other gaps. This ensures a supply of electrons released from the gap to initiate breakdown during the short period when the gaps are subjected to the overvoltage. If the first gap is not electronically triggered, the

consistency of its firing and stability of breakdown and therefore output voltage is improved by providing ultraviolet illumination for the first gap. [2]

As it can be observed by now, operating such multistage impulse generators consists in charging several capacitors, and then connecting them in series through spark gaps, obtaining so the front of the wave, which is then applied on the tested object. The maximum amplitude of voltage impulse is obtained when all capacitor are fully charged and series connected. For this to happen almost simultaneous flashover must occur on all spark gaps. This condition is achieved only when the first flashover occurs at the lower spark gap of the generator. This will happen only if the distance between the spheres of the lower spark gap is smaller than for the rest of the generator's spark gaps, as it was described previously. Such operating mode of the multistage generator presume a lack of control over the amplitude of the impulse voltage, as the amplitude of the voltage is function of the distance between the sphere gaps. Precise distances between the sphere gaps are very hard to be established, due to numerous mechanical components involved.

In order to overcome this disadvantage, the flashover of the lower spark gaps is electronically forced, due to a special construction of the lower spark gap spheres. The special construction of the controlled spark gap is presented in the figure below:

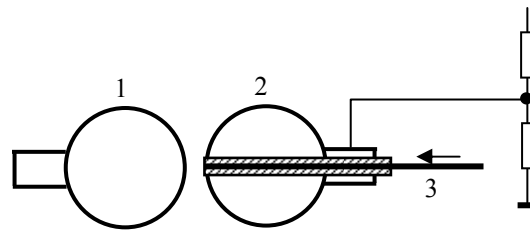


**Fig.1.10.** *Controlled spark gap special construction*

A trigger electrode (3) with the shape of a metal rod is located inside of the sphere (2), and insulated from the main electrode by an annular clearance. From an electronic circuit a voltage pulse is sent between the trigger and the main electrode, sufficient enough to breakdown the annular clearance. The ionization of the discharge and the disturbances of the field in the main gap causes its complete breakdown. This breakdown initiates the breakdown of gaps  $G$  of the other stages of the multistage generator. Thus the instant of generating the impulse can be controlled.

## II. Temporary Overvoltages in Power Grids

### II.1. Power transmission grids equivalent schemes [3]

The analytical approach of the overvoltage implies in the first stage the preparation of the equivalent scheme of the analyzed network. Temporary overvoltages have a relatively great duration and low amortization, thus the analyze will concern only the steady-state regime, at the industrial frequency.

In order to explain how the equivalent scheme must be designed, in Figure 2.1 the single-line scheme of a power network is presented. Obviously some simplifications are considered as the analyzed grid doesn't have a complex structure, and not all of the grid's switches are represented. The presented switches suggest some typically configurations of the grid, for which the temporary overvoltages will be treated.

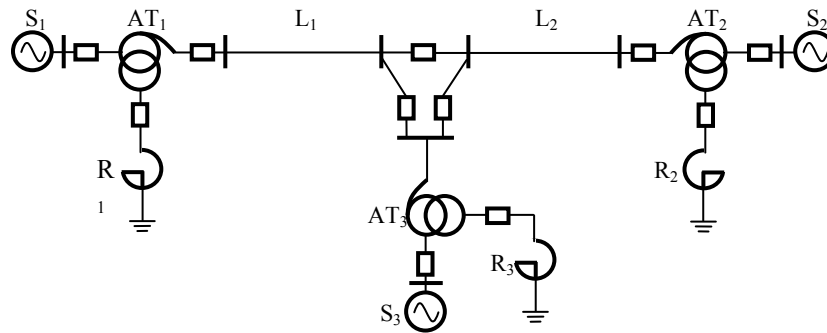


**Fig.2.1** Simplified single-line scheme of an electrical transmission grid:  $S_1, S_2, S_3$  – sources of the system;  $AT_1, AT_2, AT_{13}$  – auto-transformers;  $L_1, L_2$  – electrical lines;  $R_1, R_2, R_3$  – transversal compensation reactors.

In order to create the equivalent scheme of the electrical network, every component of the system must be replaced with an equivalent electrical circuit, adapted to the regime to be analyzed. In case of studying temporary overvoltages due to Ferranti effect, only the positive sequence scheme must be prepared. For the other types of temporary overvoltages, such as those imposed by the unbalanced shortcircuit and faults, the negative and the zero sequence schemes by must be prepared too.

A brief description of the equivalent circuits of the power grid components is presented below, all the parameters included being reported to the highest value of the maximum voltage level of the grid,  $V_m$ .

### II.1.1. Sources

In positive sequence schemes, the sources of the grid are generally represented by a positive sequence phasors system, having the module equal with the electromotive voltage of the source ( $E$ ), and by its internal impedance. If the losses are neglected, the impedance is composed only by the internal inductive reactance of the source, ( $X_{intern}$  – Fig.2.2). For power subsystems the internal inductive reactance is represented by the shortcircuit reactance ( $X_{SC}$ ), calculated according to the shortcircuit power of the upstream power subsystem ( $S_{SC}$ ):

$$X_{sc} = \frac{V_m^2}{S_{sc}} \quad (2.1)$$

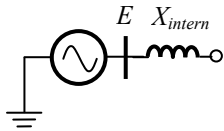


**Fig.2.2.** Direct sequence equivalent scheme of a power source

For negative and zero sequence schemes, the sources are replaced only with the specific sequence internal reactance. This way of representing occurs due to the fact that no negative voltage sources exists on the fundamental harmonic, as it is the case on higher harmonics.

In case of synchronous generators, the relation between the values of the internal reactance, calculated on the three sequences, is presented below:

$$X_{Gn} < X_{Gp} < X_{G0} \quad (2.2)$$

For power subsystems with high power, the negative sequence reactance is equal with positive sequence one, and the zero sequence reactance is about 5 per cent greater.

### II.1.2. Transformers and autotransformers

Such equipments are usually replaced in equivalent schemes with their classical „T”, „Γ” or „Γ- upside-down” diagrams. Through the elements of the scheme are represented all the process that occur in transformers, such as magnetization, dispersion, copper losses, iron core losses. Autotransformers and some transformers which are in use in the electrical transmission power grid, have usually three windings with one in delta connection. For such transformers, the „T” equivalent diagram is presented in Figure 2.3.

In case of bigger transformers the active component of the shortcircuit voltage is much smaller than the reactive component, thus comparing with the equivalent dispersion reactances, the  $R_1$ ,  $R_2$  and  $R_3$  resistances can be neglected. Also  $R_m$  resistance can be neglected, comparing with  $X_m$  reactance. Thus simplified equivalent schemes can be used, such as that shown in Fig. 2.3.b.

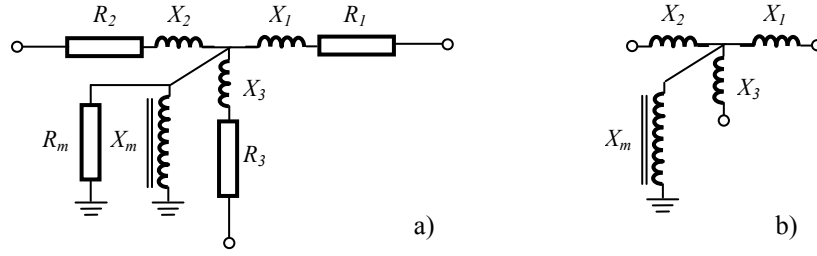


**Fig.2.3.** Three windings transformer equivalent diagram: a – losses considered; b – losses neglected;  $R_1, R_2, R_3$  – copper losses specific resistances;  $R_m$  – iron core losses specific resistance;  $X_1, X_2, X_3$  – dispersion reactances;  $X_{1m}$  – magnetization reactance.

If power losses are neglected, then the dispersion reactances can be determined with the following relation:

$$X_i = \frac{V_{sc,i}}{100} \cdot \frac{V_m^2}{S_{n,i}}, \quad i=1, 2, 3 \quad (2.3)$$

where  $V_{sc,i}$  is the shortcircuit voltage, reported to each winding, and  $S_{n,i}$  is the rated power of each winding. Shortcircuit voltages can be calculated with relation (2.4):

$$\begin{cases} V_{sc,1} = \frac{V_{sc,1-2} + V_{sc,3-1} - V_{sc,2-3}}{2} \\ V_{sc,2} = \frac{V_{sc,1-2} + V_{sc,2-3} - V_{sc,3-1}}{2} \\ V_{sc,3} = \frac{V_{sc,3-1} + V_{sc,2-3} - V_{sc,1-2}}{2} \end{cases} \quad (2.4)$$

where  $V_{sc, 1-2}$ ,  $V_{sc, 2-3}$ ,  $V_{sc, 3-1}$ , are determined from shortcircuit tests carried out on sets of 2 windings, the third remaining without load.

Magnetization reactance can be determined with the following relation:

$$X_m = \frac{100}{I_{0,\%}} \cdot \frac{V_m^2}{S_n} \quad (2.5)$$

where  $I_{0,\%}$  represents the current in case of no load, in per cents from the rated current, and  $S_n$  is the rated power of the transformer.

Negative sequence scheme is identical with the positive one, having the same values of the parameters, while the parameters of the zero sequence diagram depend on the constructive type and the wiring diagram of the transformers. In function of the wiring diagram, the zero sequence reactance can be determined using one of this relations:

$$\begin{aligned}
- \mathbf{Y}_0\mathbf{YD} &\rightarrow X_h = X_1 + X_3; \\
- \mathbf{Y}_0\mathbf{Y}_0\mathbf{D} &\rightarrow X_h = X_1 + X_2; \\
- \mathbf{Y}_0\mathbf{DD} &\rightarrow X_h = X_1 + \frac{X_2 X_3}{X_2 + X_3},
\end{aligned}
\tag{2.6}$$

$X_1, X_2$  and  $X_3$  being the positive sequence dispersion inductances.

The existence of a delta wiring connection or a star connection with isolated neutral represents a interruption point in the zero sequence diagram.

### II.1.3. Electrical lines

Considering the constructive type of the line, the rated voltage, and the type of the regime to be analyzed, there are different possibilities for replacing an electrical line in the equivalent scheme. For distribution systems, unique „T” or „II” circuits with concentrated elements and nominal parameters are generally used, in case of long electrical lines, such modeling implies unacceptable large errors. Although chains of circuits can be used for long lines, each cuadripol modeling a section of 50 -100 km of the line, such an approach leads to very complex equivalent diagrams.

In order to avoid such disadvantages, long electrical lines are replaced with distributed parameters circuits, a model of such circuit being presented in the figure below:

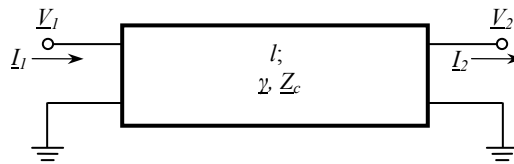


**Fig.2.4.** Equivalent diagram of a distributed parameters circuit

where:  $V_1, V_2$  and  $I_1, I_2$  represents the voltage and the current at the beginning and the end of the line,  $l$  is the length of the line,  $\underline{\gamma}$  is the complex propagation constant, and  $\underline{Z}_c$  is the characteristic impedance of the line.

Although the variation of the voltage and the current is described by some second order differential equations with partial differences, in practical calculations, the relationship between voltage and current at the ends of an electrical line, is given by a particular forms of the long lines equations, described in relation (2.7):

$$\begin{cases}
\underline{V}_1 = \underline{V}_2 \cdot \underline{ch}\underline{\gamma}l + \underline{Z}_c \underline{I}_2 \cdot \underline{sh}\underline{\gamma}l \\
\underline{I}_1 = \frac{\underline{V}_2}{\underline{Z}_c} \cdot \underline{sh}\underline{\gamma}l + \underline{I}_2 \cdot \underline{ch}\underline{\gamma}l
\end{cases}
\tag{2.7}$$

The propagation parameters are given by the following relations:

$$\underline{Z}_c = \underline{Y}_c^{-1} = \sqrt{\frac{\underline{Z}_0}{\underline{Y}_0}}; \quad \underline{\gamma} = \sqrt{\underline{Z}_0 \underline{Y}_0} = \alpha + j\beta \quad (2.8)$$

where  $\underline{Z}_0$  and  $\underline{Y}_0$  are line parameters,  $\alpha$  is the attenuation constant and  $\beta$  the phase constant.

If transversal and longitudinal losses are neglected ( $R = 0$  and  $G = 0$ ), as it can be accepted in the case of relative short electric lines, and neglecting also the corona discharge, then the attenuation constant becomes null, and the equations (2.7) can be written as following:

$$\begin{cases} \underline{V}_1 = \underline{V}_2 \cdot \cos \beta l + jZ_0 \underline{I}_2 \cdot \sin \beta l \\ \underline{I}_1 = j \frac{\underline{V}_2}{Z_0} \cdot \sin \beta l + \underline{I}_2 \cdot \cos \beta l \end{cases} \quad (2.9)$$

where  $Z_0$  is the characteristic impedance of the line, considered without losses.

If the losses can't be neglected  $R \neq 0$ , as it is the case of very long electrical lines, the propagation parameters can be calculated with the relations presented below:

$$\begin{cases} \alpha = \frac{R}{2Z_0}; & \beta = \omega \sqrt{LC}; \\ \underline{Z}_c = Z_0 \left( 1 - j \frac{\alpha}{\beta} \right); & \underline{\gamma} = \alpha + j\beta \end{cases} \quad (2.10)$$

When the voltage increases with 15 ÷ 20 per cents over the peak value of the highest voltage of the grid, corona discharge appears automatically. In such situations, the transversal parameters of the line are modified, the increasing of the capacity and the conductance loss depending on instantaneous value of the voltage. Thus the line can not be replaced by a single circuit, but through a chain of circuits, the length modeled by each circuit being small enough, so that the voltage can be considered constant along all the length of the modeled section of the line.

## II.2. Temporary overvoltages due to capacitive effect

Such overvoltages analysis are carried out in a symmetrical regime, references to a single phase being enough. Thus, only the positive sequence equivalent diagram of the analyzed grid must be designed.

An analytical approach of such type of overvoltages involves determining the relative voltage increase on the power grid lines, and the growth of the voltage at the beginning of the lines, reported to the electromotive voltage of the equivalent source.

For exemplification, a section of a power grid is considered, and presented in figure below:

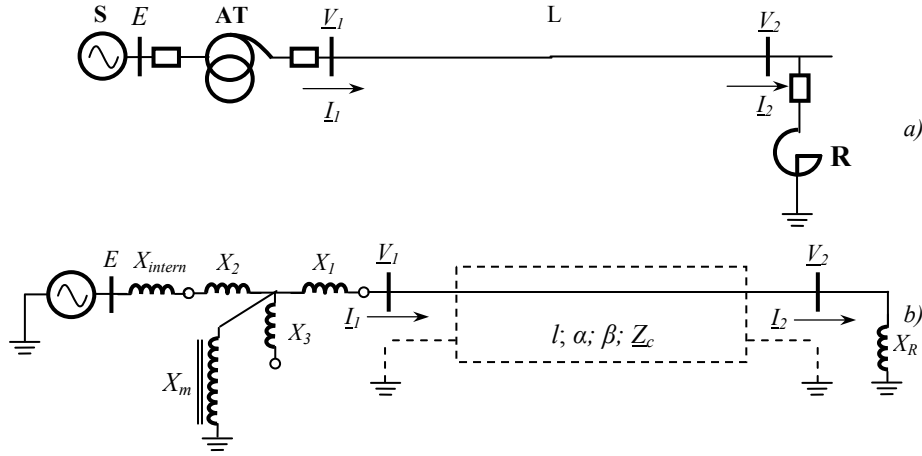


**Fig.2.5.** Single-line diagram of a section of a power transmission grid (a) and its own positive sequence equivalent scheme (b)

If the influence of the magnetization reactance of the autotransformer is neglected, then the global source reactance is:

$$X_s = X_{intern} + X_2 + X_1 \quad (2.11)$$

In order to determine the relative voltage increase on the line, first equation of the system (2.7) must be used, along with a relation to describe current  $I_2$ . Thus two situations can be considered:

- If the shunt reactor (**R**) is disconnected:

$$\begin{cases} \underline{V}_1 = \underline{V}_2 \cdot \underline{ch}\gamma l + \underline{Z}_c \underline{I}_2 \cdot \underline{sh}\gamma l \\ \underline{I}_2 = 0 \end{cases} \quad (2.12)$$

- If the shunt reactor (**R**) is connected:

$$\begin{cases} \underline{V}_1 = \underline{V}_2 \cdot \underline{ch}\gamma l + \underline{Z}_c \underline{I}_2 \cdot \underline{sh}\gamma l \\ \underline{I}_2 = \frac{\underline{V}_2}{jX_R} \end{cases} \quad (2.13)$$

For both of the situations described above, the overvoltage factor can be determined with the following relations:

$$k_1 = \left| \frac{V_2}{V_1} \right| = \frac{1}{|ch\gamma l|} \quad \text{and} \quad k_1 = \left| \frac{V_2}{V_1} \right| = \frac{1}{\left| ch\gamma l + \frac{Z_c}{jX_R} sh\gamma l \right|} \quad \text{respectively} \quad (2.14)$$

If all losses are neglected ( $\alpha = 0$ ), then relations (2.14) can be written as (2.15):

$$k_1 = \frac{V_2}{V_1} = \frac{1}{\cos \beta l} \quad \text{and} \quad k_1 = \frac{V_2}{V_1} = \frac{1}{\cos \beta l + \frac{Z_0}{X_R} \sin \beta l} \quad \text{respectively} \quad (2.15)$$

The voltage growth at the beginning of the line, reported to the electromotive voltage of the source, can be determined using an uniform equivalent electrical diagram with lumped parameters, obtained by replacing the line with his input impedance  $Z_i$ , as described in the figure below:

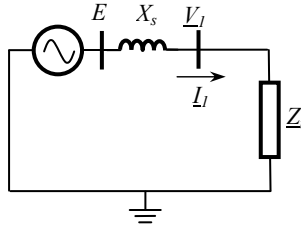


**Fig.2.6.** Uniform electrical diagram used for voltage growth determination, at the beginning of the line

If all power losses are neglected, the equations systems requested in order to determine the computing relation of the input impedance  $Z_i$ , of the line, are further presented :

- If the shunt reactor (**R**) is disconnected:

$$\begin{cases} V_1 = V_2 \cdot \cos \beta l + jZ_0 I_2 \cdot \sin \beta l \\ I_1 = j \frac{V_2}{Z_0} \cdot \sin \beta l + I_2 \cdot \cos \beta l \\ I_2 = 0 \end{cases} \quad (2.16)$$

- If the shunt reactor (**R**) is connected:

$$\begin{cases} V_1 = V_2 \cdot \cos \beta l + jZ_0 I_2 \cdot \sin \beta l \\ I_1 = j \frac{V_2}{Z_0} \cdot \sin \beta l + I_2 \cdot \cos \beta l \\ I_2 = \frac{V_2}{jX_R} \end{cases} \quad (2.17)$$

The computing relation of the input impedance of a line operating without load, can be obtained from the system of equations (2.16), and is presented below:

$$\underline{Z}_i = \frac{V_1}{I_1} = -jZ_0 \cdot \text{ctg}\beta l \quad (2.18)$$

If the shunt reactors connected at the end of the line, the value of line's input impedance is determined from system (2.17), and it can be computed with the following expression:

$$\underline{Z}_i = \frac{V_1}{I_1} = -jZ_0 \cdot \frac{1 + \frac{Z_0}{X_R} \cdot \text{tg}\beta l}{1 - \frac{Z_0}{X_R} \cdot \text{ctg}\beta l} \cdot \text{ctg}\beta l = -jZ'_0 \cdot \text{ctg}\beta l \quad (2.19)$$

Considering the circuit presented in Fig.2.6. operating in a steady-state regime, then the second Theorem of Kirchhoff and the Ohm's Law can be applied, obtaining the following system:

$$\begin{cases} E = jX_s I_1 + V_1 \\ I_1 = \frac{V_1}{\underline{Z}_i} \end{cases} \quad (2.20)$$

By resolving the system (2.20), the computing relation of the voltage growth at the beginning of the line is obtained:

$$k_2 = \left| \frac{V_1}{E} \right| = \frac{1}{1 - \frac{X_s}{Z_0} \cdot \text{tg}\beta l} \quad (2.21)$$

The relation presented above corresponds to the situation when the analyzed line is operating without load. If a shunt reactor is connected at the end of the line, then instead of the characteristic impedance of the line without losses,  $Z_0$ , equivalent impedance  $Z'_0$ , must be considered and its value can be determine with relation (2.19).

The global overvoltage factor, which reflects the real stress over the line's insulation is given by the following relation:

$$k = \frac{V_2}{E} = \frac{V_2}{V_1} \cdot \frac{V_1}{E} = k_1 \cdot k_2 \quad (2.22)$$

### II.3. Temporary overvoltages due unbalanced shortcircuits

When unbalanced shortcircuits occurs on the power transmission lines, usually dangerous overcurrents and overvoltages appear. Transient overvoltages generated by the fault's appearance and the line's disconnection have a significant 50 Hz component, which in some situations can become unacceptable high. Although such regimes last for a short period of time, the amplitude of the fundamental harmonic component can be determined as a steady-state regime temporary overvoltage.

When disconnecting a line the switches at the end of it, usually don't operate simultaneous on all three phases, thus the healthy phase(s) operate for a short period of time without any load. This leads to significant overvoltages, due to the unbalanced shortcircuit regime of the line, and also because of the voltage increasing on the healthy phase(s) given by the capacitive effect (Ferranti effect).

Using the symmetrical components method, the computing relations of the phase to ground voltage at the point where shortcircuit occurred, are determined:

- For single-phase shortcircuit:

$$\begin{cases} V_A = 0 \\ \frac{V_{B,C}}{V} = -\frac{3}{2} \cdot \frac{Z_h}{2Z_d + Z_h} \mu j \frac{\sqrt{3}}{2} \end{cases} \quad (2.23)$$

- For double-phase to ground shortcircuit:

$$\begin{cases} \frac{V_A}{V} = \frac{3Z_h}{Z_d + 2Z_h} \\ V_{B,C} = 0 \end{cases} \quad (2.24)$$

Where:  $V$  – the voltage at the point where shortcircuit occurred, in the previous regime to the shortcircuit;  $Z_d$ ,  $Z_h$  – positive and zero sequence impedance, determined in relation to the point where shortcircuit occurred.

For the power transmission lines, the voltage level must be known not only at the point where shortcircuit occurs, but also in other points, like the power stations at the ends of the lines. Thus the computing relations for phase to ground voltages in any other points of the power grid are:

- For single-phase shortcircuit:

$$\begin{cases} \frac{V'_A}{V} = \frac{V'}{V} - \frac{2k_d \cdot Z_d + k_h \cdot Z_h}{2Z_d + Z_h} \\ \frac{V'_{B,C}}{V} = \left( -\frac{1}{2} \mu j \frac{\sqrt{3}}{2} \right) \cdot \frac{V'}{V} - \frac{k_h \cdot Z_h - k_d \cdot Z_d}{2Z_d + Z_h} \end{cases} \quad (2.25)$$

- For double-phase to ground shortcircuit:

$$\begin{cases} \frac{V'_A}{V} = \frac{V'}{V} + \frac{k_h \cdot Z_h - k_d \cdot Z_d}{Z_d + 2Z_h} \\ \frac{V'_{B,C}}{V} = \left( -\frac{1}{2} \mu j \frac{\sqrt{3}}{2} \right) \cdot \frac{V'}{V} + \frac{k_h \cdot Z_h + 0,5k_d \cdot Z_d}{Z_d + 2Z_h} \pm j \frac{\sqrt{3}}{2} \cdot k_d \end{cases} \quad (2.26)$$

Where:  $\underline{U}'$  – represents the voltage in the chosen point, in the previous regime to the shortcircuit;  $k_d$  and  $k_h$  – positive and zero sequence reporting coefficients of the voltage from the computing point and the voltage at point of the shortcircuit.

As the long electrical lines are replaced by equivalent circuits with distributed parameters, the computing relations of the positive and zero sequence equivalent impedances, and also of the reporting coefficients, are determined using the long lines equations. Thus the equivalent impedance is known as the *shortcircuit impedance* and it is computed similar as a input impedance, when the shortcircuit is considered to be the source of the equivalent diagram. As example, the equivalent scheme needed for shortcircuit impedance determination of the single-line diagram presented in Fig.2.5.a, is given in the figure below:

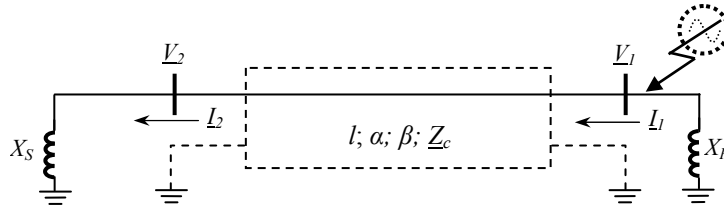


**Fig.2.7.** Equivalent electrical scheme requested for shortcircuit impedance determination, when the shortcircuit occurred at the end of a power transmission line

In order to keep the form of the long lines equations, in the equivalent diagram presented above, the voltage and current at the end of the line were noted in the opposite direction in relation to the ends of the line, than in Fig.2.5.b.

If all power losses are neglected and the shunt reactor is disconnected, the computing relation of the shortcircuit impedance is determined from the following system of equations:

$$\begin{cases} V_1 = V_2 \cdot \cos \beta l + jZ_0 I_2 \cdot \sin \beta l \\ I_1 = j \frac{V_2}{Z_0} \cdot \sin \beta l + I_2 \cdot \cos \beta l \\ I_2 = \frac{V_2}{jX_S} \end{cases} \quad (2.27)$$

the shortcircuit impedance being calculated with expression presented below:

$$\underline{Z}_{sc} = \frac{V_1}{\underline{I}_1} = jZ_0 \cdot \operatorname{tg} \left( \beta l + \operatorname{arctg} \frac{X_S}{Z_0} \right) \quad (2.28)$$

Relation (2.28) is customized for both positive and zero sequence, the specific reactances being determined with the following relations:

$$\begin{cases} X_d = X_{sc,d} = Z_{0,d} \cdot \operatorname{tg} \left( \beta_d l + \operatorname{arctg} \frac{X_{S,d}}{Z_{0,d}} \right) \\ X_h = X_{sc,h} = Z_{0,h} \cdot \operatorname{tg} \left( \beta_h l + \operatorname{arctg} \frac{X_{S,h}}{Z_{0,h}} \right) \end{cases} \quad (2.29)$$

If the shunt reactor is connected, then the current  $\underline{I}_l$  has two components: one who travels to the line ( $\underline{I}_{l,1}$ ), and one that closes through the shunt reactor reactance ( $\underline{I}_{l,2}$ ). The second equations from (2.27) is valid for current ( $\underline{I}_{l,1}$ ), while for shortcircuit impedance determination two more equations are needed. One of them results when Ohm's Law is applied for the  $X_R$  circuit reactance, and the second one is deduced by applying the first Law of Kirchhoff in the shortcircuit point. The computing relation of the shortcircuit impedance, when the shunt reactor is connected, is obtained by solving this new system of equations, and the relation is presented below:

$$\underline{Z}_{sc} = \frac{V_1}{\underline{I}_1} = \frac{jZ_0 \cdot \operatorname{tg} \left( \beta l + \operatorname{arctg} \frac{X_S}{Z_0} \right) \cdot jX_R}{jZ_0 \cdot \operatorname{tg} \left( \beta l + \operatorname{arctg} \frac{X_S}{Z_0} \right) + jX_R} = jZ_0 \cdot \frac{\operatorname{tg} \left( \beta l + \operatorname{arctg} \frac{X_S}{Z_0} \right)}{1 + \frac{Z_0}{X_R} \cdot \operatorname{tg} \left( \beta l + \operatorname{arctg} \frac{X_S}{Z_0} \right)} \quad (2.30)$$

From the last relation it is obvious that the shortcircuit impedance is obtained as an equivalent impedance formed by the equivalent impedance of the circuit without shunt reactor, connected in parallel with the shunt reactor impedance.

If the voltage at the shortcircuit point, at some time before shortcircuit, is known then the phase to ground voltage at the shortcircuit point can be determined with the relations presented until now. For calculating the voltage at the beginning of the line, the associated reporting coefficients must be determined first. Considering the notations made in Fig.2.7., and neglecting all power losses, the reporting coefficients can be determined from the following system:

$$\begin{cases} \underline{V}_1 = \underline{V}_2 \cdot \cos \beta l + jZ_0 \underline{I}_2 \cdot \sin \beta l \\ \underline{I}_2 = \frac{\underline{V}_2}{jX_S} \\ k = \frac{\underline{V}_2}{U_1} \end{cases} \quad (2.31)$$

No matter if the shunt reactor is connected or disconnected, the reporting coefficients can be calculated with the relation presented below:

$$k = \frac{1}{\cos \beta l + \frac{Z_0}{X_s} \cdot \sin \beta l} \quad (2.32)$$

Customizing the last expression for the positive and zero sequence, following relations are obtained:

$$k_d = \frac{1}{\cos \beta_d l + \frac{Z_{0,d}}{X_{S,d}} \cdot \sin \beta_d l} \quad \text{and} \quad k_h = \frac{1}{\cos \beta_h l + \frac{Z_{0,h}}{X_{S,h}} \cdot \sin \beta_h l} \quad (2.33)$$

Thus in case of an unbalanced shortcircuit on a power transmission line, all computing relation of the voltage in different points of the line were determined.

## II.4. Temporary overvoltages due unbalanced faults

In case of the refusal of an equipment to perform a switching operation, or in case of disconnection of a phase conductor, the temporary operation of the grid with an incomplete number of phases, can lead to significant overvoltages, due to the occurrence of the resonance at the industrial frequency, or due to ferro-resonance phenomenon.

If the transformer's magnetization reactances are neglected, and thus the possibility of magnetic iron core saturation, the equivalent diagram contains only linear components. For this type of electrical scheme, resonance overvoltage can be determined. Even more, in case that such unbalanced faults occurs when the power line has no load, significant increases of the voltage must be expected due to the overlapping effects.

For example such regimes can be analyzed for the single-line diagram of an power grid, presented in Figure 2.8. In this situation the unbalanced fault is generated by the autotransformer upstream switch.

Using the symmetrical components method, the following computing relations of the phase to ground voltage are determined:

a) Single phase disconnection:

- voltages at the fault location, before that point:

$$\begin{cases} \frac{V_{1,A}''}{E} = 1 + \frac{Z_{int,h} - Z_{int,d}}{Z_{1d} + 2Z_{1h}} \\ \frac{V_{1,B;C}''}{E} = \left( -\frac{1}{2} \mu j \frac{\sqrt{3}}{2} \right) \cdot \frac{Z_{id}}{Z_{1d}} + \frac{Z_{id} Z_{int,h} - Z_{int,d} Z_{ih}}{Z_{1d} \cdot (Z_{1d} + 2Z_{1h})} \end{cases} \quad (2.34)$$

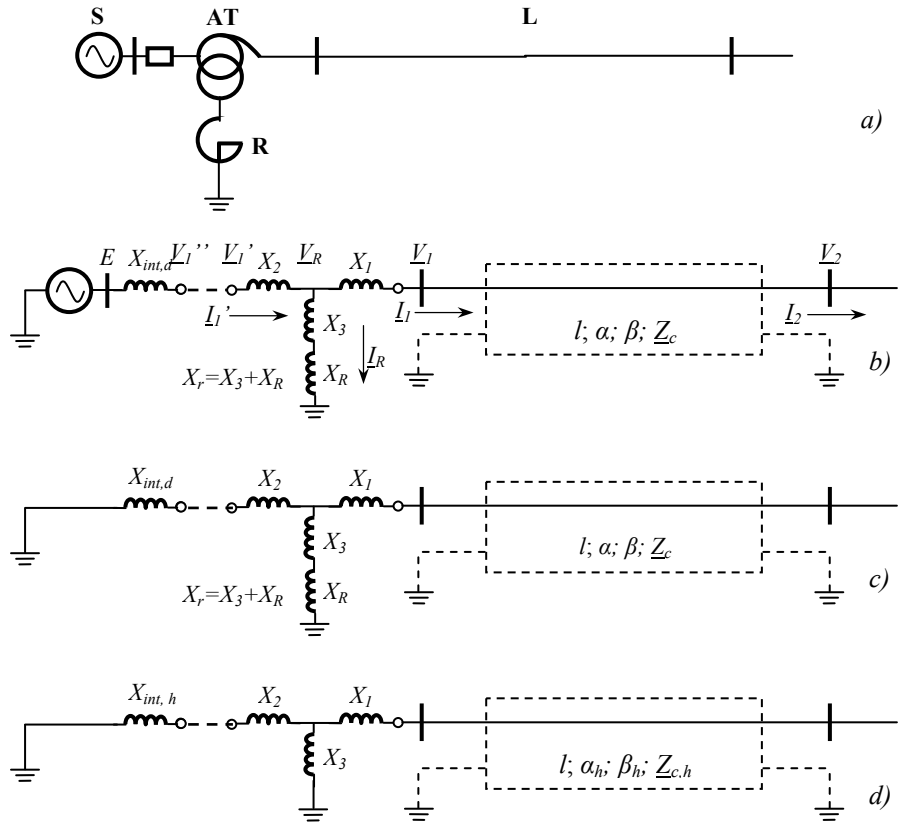


Fig.2.8. (a) - Single-line diagram; (b), (c), (d) – positive, negative and zero sequence equivalent scheme for unbalanced faults analyzing

- voltages at the fault location, after that point:

$$\begin{cases} \frac{V'_{1,A}}{E} = \frac{Z_{id} - Z_{ih}}{Z_{1d} + 2Z_{1h}} \\ \frac{V'_{1,B;C}}{E} = \frac{V''_{1,B;C}}{E} \end{cases} \quad (2.35)$$

- phase to ground voltage in any point of the line:

$$\begin{cases} \frac{V_{2,A}}{E} = \frac{k_d Z_{id} - k_h Z_{ih}}{Z_{1d} + 2Z_{1h}} \\ \frac{V_{2,B;C}}{E} = -\frac{k_h Z_{ih} + 0,5k_d Z_{id}}{Z_{1d} + 2Z_{1h}} \mu j \frac{\sqrt{3}}{2} k_d \frac{Z_{id}}{Z_{1d}} \end{cases} \quad (2.36)$$

b) Double - phase disconnection

- voltages at the fault location, before that point:

$$\begin{cases} \frac{V_{1,A}''}{E} = \frac{2\underline{Z}_{id} + \underline{Z}_{ih}}{2\underline{Z}_{1d} + \underline{Z}_{1h}} \\ \frac{V_{1,B;C}''}{E} = \left( -\frac{1}{2} \mu j \frac{\sqrt{3}}{2} \right) - \frac{\underline{Z}_{int,h} - \underline{Z}_{int,d}}{2\underline{Z}_{1d} + \underline{Z}_{1h}} \end{cases} \quad (2.37)$$

- voltages at the fault location, after that point:

$$\begin{cases} \frac{V_{1,A}'}{E} = \frac{V_{1,A}''}{E} \\ \frac{V_{1,B;C}'}{E} = \frac{\underline{Z}_{ih} - \underline{Z}_{id}}{2\underline{Z}_{1d} + \underline{Z}_{1h}} \end{cases} \quad (2.38)$$

- phase to ground voltage in any point of the line:

$$\begin{cases} \frac{V_{2,A}}{E} = \frac{2k_d \underline{Z}_{id} + k_h \underline{Z}_{ih}}{2\underline{Z}_{1d} + \underline{Z}_{1h}} \\ \frac{V_{2,B;C}}{E} = \frac{k_h \underline{Z}_{ih} - k_d \underline{Z}_{id}}{2\underline{Z}_{1d} + \underline{Z}_{1h}} \end{cases} \quad (2.39)$$

Where:

- $\underline{Z}_{int,d}$  and  $\underline{Z}_{int,h}$  – positive and zero sequence internal impedance of the source;
- $\underline{Z}_{id}$  and  $\underline{Z}_{ih}$  – positive and zero sequence input impedance of the circuit before the unbalanced fault location;
- $k_d$  and  $k_h$  – positive and zero sequence reporting coefficients of the voltages from the chosen computing point and from the unbalanced fault location;
- $\underline{Z}_{1d}$  and  $\underline{Z}_{1h}$  – equivalent impedances given by the following relations:

$$\underline{Z}_{1d} = \underline{Z}_{int,d} + \underline{Z}_{id} \quad \text{and} \quad \underline{Z}_{1h} = \underline{Z}_{int,h} + \underline{Z}_{ih} \quad (2.40)$$

Considering the notations made in Fig. 2.8., the input impedance in relation with the fault location can be determined from the following equivalent electrical scheme, with lumped parameters:

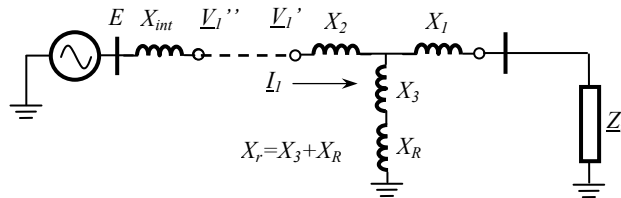


**Fig.2.9.** Equivalent diagram for the input impedance determination in case of an unbalanced fault generated by the switch from a transformer-line block diagram

The input impedance in relation with fault location can be determined using the relation presented below:

$$\underline{Z}_i = \frac{V_1'}{I_1} = jX_2 + \frac{jX_r \cdot (jX_1 + \underline{Z}_{il})}{jX_r + jX_1 + \underline{Z}_{il}} \quad (2.41)$$

Where  $\underline{Z}_{il}$  is the input impedance of the line, and it can be determined as it was presented in the paragraph II.2.

If the all power losses are neglected and the line is operating without any load, the input impedance in relation with fault location, can be obtained using the relation below:

$$\underline{Z}_i = j \cdot \left[ X_2 + \frac{(X_3 + X_R) \cdot (X_1 - Z_0 \cdot \text{ctg} \beta l)}{X_3 + X_R + X_1 - Z_0 \cdot \text{ctg} \beta l} \right] \quad (2.42)$$

Customizing the relation (2.42), the input impedance relation for positive and zero sequence are obtained:

$$\begin{cases} \underline{Z}_{id} = j \cdot \left[ X_2 + \frac{(X_3 + X_R) \cdot (X_1 - Z_{0,d} \cdot \text{ctg} \beta_d l)}{X_3 + X_R + X_1 - Z_{0,d} \cdot \text{ctg} \beta_d l} \right] = j \cdot X_{id} \\ \underline{Z}_{ih} = j \cdot \left[ X_2 + \frac{X_3 \cdot (X_1 - Z_{0,h} \cdot \text{ctg} \beta_h l)}{X_3 + X_1 - Z_{0,h} \cdot \text{ctg} \beta_h l} \right] = j \cdot X_{ih} \end{cases} \quad (2.43)$$

When a shunt reactor is connected at the end of the line, the input impedance of the line from relation (2.41) is replaced with that one from relation (2.19).

Similar to the case of unbalanced shortcircuits, the voltage level must be determined also in other nodes of the line. In this sense relations (2.36) and (2.39) can be used, but first the reporting coefficients must be determined. Considering the notations made in Fig.2.8., the computing relation of the reporting coefficient can be determined from the system presented below:

$$\begin{cases} V_1 = V_2 \cos \beta l + jZ_0 I_2 \sin \beta l \\ I_1 = j \frac{V_2}{Z_0} \sin \beta l + I_2 \cos \beta l \\ I_2 = 0 \\ V_R = V_1 + jX_1 I_1 \\ V_1' = V_R + jX_1 I_1' \\ I_R = \frac{V_R}{jX_r} \\ I_1' = I_1 + I_R \end{cases} \quad (2.44)$$

Solving the system (2.44) in sense of determining the ratio between the voltage at the end of the line, and at the fault location, leads to the general computing relation of the reporting coefficients:

$$k = \left| \frac{V_2}{V_1} \right| = \frac{1}{\cos \beta l} \cdot \frac{1}{1 + \frac{X_2}{X_r} - \frac{1}{Z_0} \cdot \left( X_1 + X_1 + \frac{X_1 X_2}{X_r} \right) \cdot \operatorname{tg} \beta l} \quad (2.45)$$

Computing relations for the positive and zero sequence reporting coefficients are obtained by customizing relation (2.45). Thus the following relations can be used:

$$\begin{cases} k_d = \frac{1}{\cos \beta_d l} \cdot \frac{1}{1 + \frac{X_2}{X_r} - \frac{1}{Z_{0,d}} \cdot \left( X_1 + X_1 + \frac{X_1 X_2}{X_r} \right) \cdot \operatorname{tg} \beta_d l} \\ k_h = \frac{1}{\cos \beta_h l} \cdot \frac{1}{1 + \frac{X_2}{X_3} - \frac{1}{Z_{0,h}} \cdot \left( X_1 + X_1 + \frac{X_1 X_2}{X_3} \right) \cdot \operatorname{tg} \beta_h l} \end{cases} \quad (2.46)$$

### III. Lightning Overvoltages

#### III.1. Lightning discharge and lightning parameters

##### III.1.1. Lightning discharge

Lightning is a natural phenomenon that has always produced much impact on humans and their societies, mainly because of its impressive appearance and the threats imposed on life and structures. Lightning discharges are in fact electrical discharges generated in the Earth's atmosphere mainly by cumulonimbus clouds.

Lightning discharges can be separated into two main categories, ground flashes and cloud flashes. Lightning discharges that make contact with ground are referred to as ground flashes and the rest are referred to as cloud flashes. Cloud flashes in turn can be divided into three types: intra-cloud flashes, air discharges and inter-cloud discharges. These different categories of lightning flashes are illustrated in Figure 3.1.a [4]. A ground flash can be divided into four categories based on the polarity of charge it brings to the ground and its point of initiation. These four categories are illustrated in Figure 3.1.b: downward negative ground flashes, downward positive ground flashes, upward positive ground flashes and upward negative ground flashes. The polarity of the flash, i.e. negative or positive, is based on the polarity of the charge brought to the ground from the

cloud. It is thought that upward lightning flashes are initiated by tall objects of heights more than  $\approx 100$  m or structures of moderate heights located on mountain and hill tops. [4].

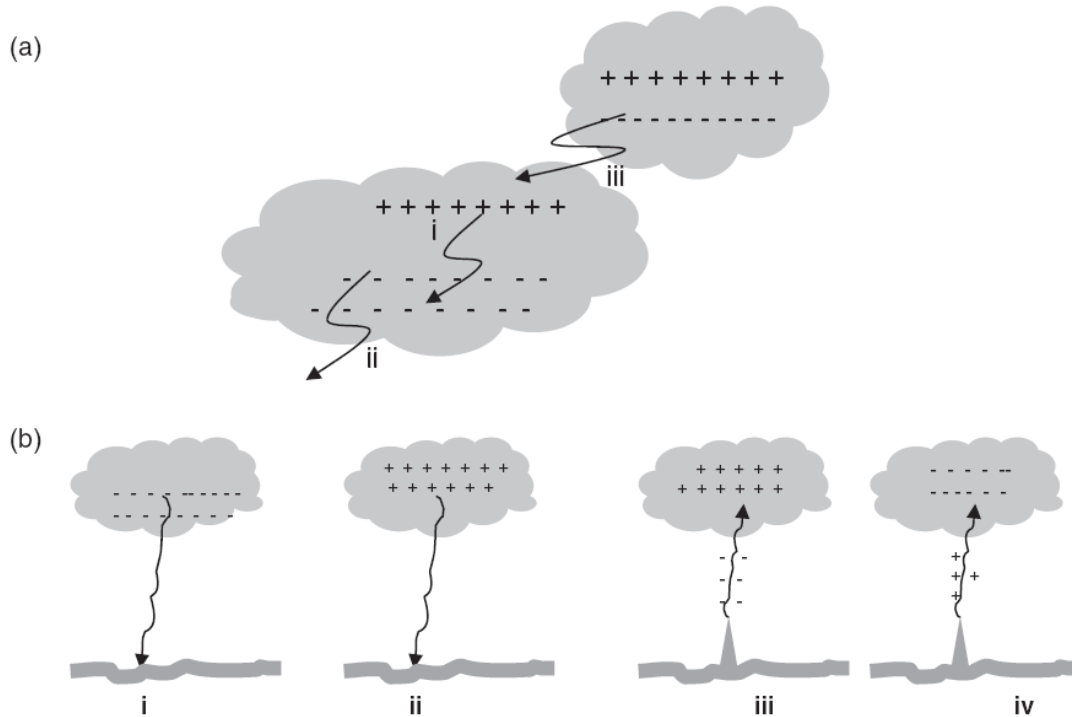


**Fig.3.1.** (a) Types of cloud flashes: (i) intra-cloud; (ii) air discharges; (iii) inter-cloud.(b) Types of ground flashes: (i) downward negative ground flashes; (ii) downward positive ground flashes; (iii) upward positive ground flashes; (iv) upward negative ground flashes.

It is believed that downward negative lightning discharges account for about 90% of all cloud-to-ground lightning, and that about 10% of cloud-to-ground lightning are downward positive lightning discharges.

A downward negative ground flash is initiated by an electrical breakdown process in the cloud called the preliminary breakdown. This process leads to the creation of a column of charge, called the stepped leader, which travels from cloud to ground in a stepped manner. Some researchers use the term preliminary breakdown to refer to both the initial electrical activity inside the cloud and the subsequent stepped leader stage. On its way towards the ground a stepped leader may give rise to several branches. As the stepped leader approaches the ground, the electric field at ground level increases steadily. When the stepped leader reaches a height of about a few hundred meters or less above ground, the electric field at the tip of the grounded structures increases to such a level that electrical discharges are initiated from them. These discharges, called connecting leaders,

travel towards the down-coming stepped leader. One of the connecting leaders may successfully bridge the gap between the ground and the down-coming stepped leader. The object that initiated the successful connecting leader is the one that will be struck by lightning. The distance between the object struck and the tip of the stepped leader at the inception of the connecting leader is called the striking distance.

The moment a connection is made between the stepped leader and ground, a wave of near-ground potential travels at a speed close to that of light along the channel towards the cloud. The current associated with this wave heats the channel to several tens of thousands of degrees Kelvin, and creates a channel pressure of 10 atm or more, which results in channel expansion, intense optical radiation, and an outward propagating shock wave that eventually becomes the thunder. This event is called the return stroke. Whenever the upward-moving return stroke front encounters a branch, there is an immediate increase in the luminosity of the channel; such events are called branch components. Although the current associated with the return stroke tends to last for a few hundred microseconds, in certain instances the return stroke current may not go to zero within this time, but may continue to flow at a low level for a few to few hundreds of milliseconds. Such long duration currents are called continuing currents. [4]

When the first return stroke ceases, the flash may end. In this case, the lightning is called a single-stroke flash. However, more often the residual first-stroke channel is traversed downwards by a leader that appears to move continuously, a dart leader. When a dart leader or dart-stepped leader approaches the ground, an attachment process similar to that described for the first stroke takes place, although it probably occurs over a shorter distance and consequently takes less time, the upward connecting-leader length being of the order of some meters. Once the bottom of the dart leader or dart-stepped leader channel is connected to the ground, the second (or any subsequent) return-stroke wave is launched upward and serves to neutralize the leader charge. The subsequent return-stroke current at ground typically rises to a peak value of 10–15 kA in less than a microsecond and decays to half-peak value in a few tens of microseconds.

The time interval between successive return strokes in a flash is usually several tens of milliseconds, although it can be as large as many hundreds of milliseconds if a long continuing current is involved and as small as one millisecond or less. The total duration of a flash is typically some hundreds of milliseconds, and the total charge lowered to ground is some tens of coulombs. The overwhelming majority of negative cloud-to-ground flashes contain more than one stroke. Although the first stroke is usually a factor 2 to 3 larger than a subsequent stroke, about one-third of multiple stroke flashes have at least one subsequent stroke that is larger than the first stroke in the flash. [5]

### III.1.2. Lightning parameters

The primary interest parameters of the lightning flash are:

- the crest current for the first and subsequent strokes;
- the wave shape of these currents;
- correlation between different current parameters;
- the number of strokes per flash;
- Flash incidence rates: the ground flash density, flashes per square km-year.

The most significant parameters of the lightning current waveform can be identified from Figure 3.2., and additional information concerning these parameters is given in Table 3.1. [4]

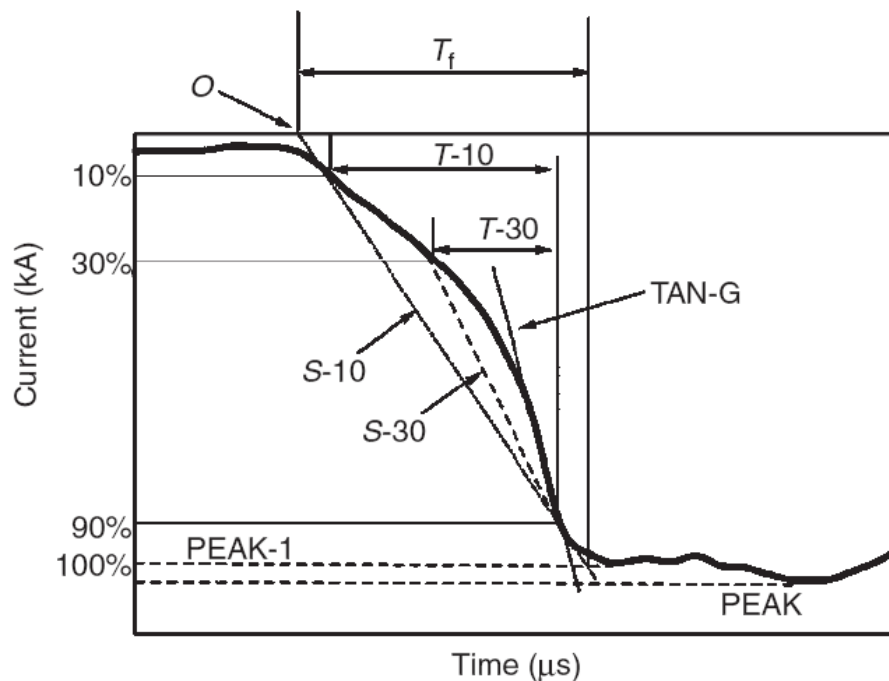


*Fig.3.2. Lightning current parameters*

Over the time many researchers proposed different values of the lightning current parameters presented in Tabel 3.1, as a result of their experimental measurements. Such values are well presented in [4].

In a statistical approach lightning current parameters can be approximated by log-normal distributions, where the logarithm of the random variable  $x$  follows the normal or Gaussian distribution. Such distributions are characterized by a medium value  $x_m$  and a standard deviation  $\beta$ . The probability density function  $p(x)$  of  $x$  of this distribution is given by the following relation:

$$p(x) = \frac{1}{\sqrt{2\pi\beta x}} e^{-0.5\left[\frac{\ln(x)-\ln(x_m)}{\beta}\right]^2} \quad (3.1)$$

**Table 3.1.** Definition of different lightning-current parameters

Parameter	Significance
PEAK (kA)	The highest current peak
$T_f$ ( $\mu$ s)	Front duration
$T_{-10}$ ( $\mu$ s)	Time between the 10% and 90% values of PEAK-1 at the wave front
$T_{-30}$ ( $\mu$ s)	Time between the 30% and 90% values of PEAK-1 at the wave front
$T_t$ ( $\mu$ s)	Stroke duration; time from the virtual zero time to the half-peak value of the wave tail
$TAN_{-10}$ ( $\text{kA } \mu\text{s}^{-1}$ )	Rate of rise at the 10% point of PEAK-1
$TAN_G$ ( $\text{kA } \mu\text{s}^{-1}$ )	Maximum rate of rise
$S_{-10}$ ( $\text{kA } \mu\text{s}^{-1}$ )	Average rate of rise between the 10% and 90% values of PEAK-1
$S_{-30}$ ( $\text{kA } \mu\text{s}^{-1}$ )	Average rate of rise between the 30% and 90% values of PEAK-1

The values of the median and standard deviation of the log-normal distribution were determined by several researchers and a complete syntheses of these values is also presented in [4]. For the peak-current distribution of the negative ground flashes the recommendation of CIGRE is generally adopted. According to this, for  $I_p \leq 20$  kA the median value is 61.1 kA and the standard deviation  $\beta = 1.33$ . For  $I_p \geq 20$  kA, the median value is 33.3 kA and the standard deviation  $\beta = 0.605$ .

As the shape and the values of different parameters of the lightning current waveform is different for each lightning strike, for practical purposes like insulation tests, a standard lightning current or voltage waveform is used. The specifications of this standard lightning waveform are well presented in paragraph I.3.

As for the other lightning parameters, the ground flash density and the number of strokes per flash, these are important parameters in lightning protection analysis. Ground flash density  $N_g$  in a given region can be estimated by counting the number of lightning flashes that strike ground in that region by using lightning flash counters, lightning location systems or using information on lightning strikes provided by satellites. However, lightning-protection engineers still use thunderstorm days to extract ground flash density because information concerning this parameter is available world wide. A thunderstorm day is normally defined as the local calendar day in which thunder is heard by meteorological observers. In the absence of better information about ground flash density it can be estimated from thunderstorm days,  $T_d$ , using an equation of the form: [4]

$$N_g = aT_d^b \text{ flashes / km}^2 \text{ year} \quad (3.2)$$

The parameters of this equation have been derived by many researchers, but the generally used formula is known as CIGRE formula for which  $a = 0.04$  and  $b = 1.25$ .

### **III.2. Protection of electrical installations against direct lightning strokes**

Direct lightning strokes represents one of the most common cause of the power systems' failures, as the power transmission lines are the electric grids' elements most exposed to lightning strokes, due their height, and their length. Power stations are also exposed due to their wide lightning collection area. Serious failures that may occur require a special focus on the protection of power systems' components against direct lightning strokes.

Usually the protection against direct lightning strokes is ensured by installing lightning protective systems, such as lightning rods or ground wires for power stations and ground wires for power transmission lines. Their role is to take on them the direct lightning strokes ensuring a minimum risk of hitting for the active parts of the power system. The protective effect of the lightning rods or ground wires can be estimated by the lightning stroke probability of penetration beside the lightning rod or ground wire. This probability can be calculated as the ratio between the number of strokes hitting the protected equipments and the total number of the strokes hitting the entire system of lightning rods and protected equipments. [6]

The minimum risk for direct lightning strokes in the active components of the power system is obtained when the protective zone given by the lightning rods or ground wires covers all those active parts. In such circumstances, the precise calculation of the protective zone is one of the most important stages in the power stations or transmission lines design.

In order to determine the dimensions of the protective zones, generated by the lightning protective systems, over the time several methods were developed, such as:

- ✓ laboratory models method;
- ✓ rolling sphere method, based on the electrogeometrical theory.

The aim of these models is to determine more precisely the point on the ground to be struck by the lightning discharge, thus facilitating optimal sizing and instalation of the lightning protective system, and thus a lower risk of screen failure. As a result of research of the last two decades, the final stage of the lightning discharge was described through a series of new mathematical models, even more complex, known under the name of leader progressive models, such as the Delleria and Garbagnati model, Rizk model, and the most recent model was proposed by Beccera and Cooray in 2006. The leader progressive models are not yet standardized, as prestigious standads like IEEE [7] and IEC [8] still recommend the rolling sphere method for the protective zone dimensions determination.

### III.2.1. Laboratory models method [6]

Nowadays the lightning protective systems of Romanian's power system' stations are designed according to the laboratory models method. This method assumes that the lightning discharge will be heading to certain structure on the ground, from a distance proportional with the height of the structure. The protective zones estimated with this method have a risk of penetration of 0.1 %, regardless the intensity of the lightning current.

Applying this classical method for sizing a system of vertical rods, or for checking an existing one, involves the following steps:

- tracing the outline of the horizontal sections through the protection zone created by lightning rod system;
- verify the absence of an uncovered area in the horizontal plane of analysis in the space between the lightning system.

The horizontal planes for which the protection efficiency is verified are those of the busbars hanging in case of power stations, or the hanging planes of the power transmission line' phase conductors. For tracing the outline of the protective zone groups of two adjacent lightning rods are considered, whether or not they have equal heights.

To establish the protective zone given by two adjacent lightning rods, the protective zone of a single vertical rod must be determined. For a single vertical rod, the protected zone has a cone shape with curves generators, as it is presented in Figure 3.3.

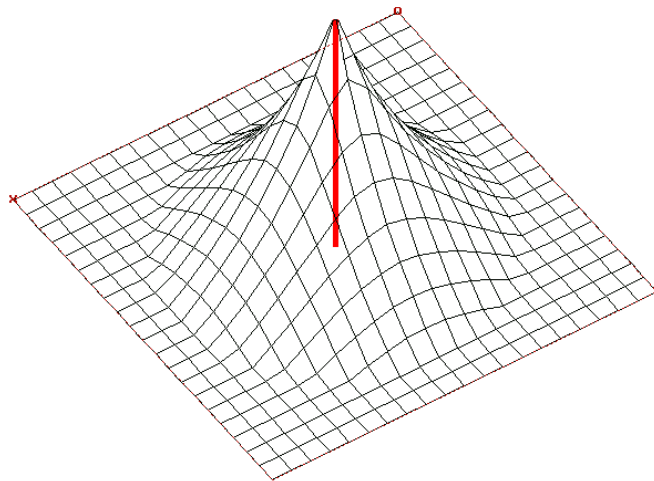


*Fig.3.3. 3D perspective of the protective zone generated by a vertical rod*

The longitudinal and cross section through the protective zone generated by a single vertical rod are presented in figure below:

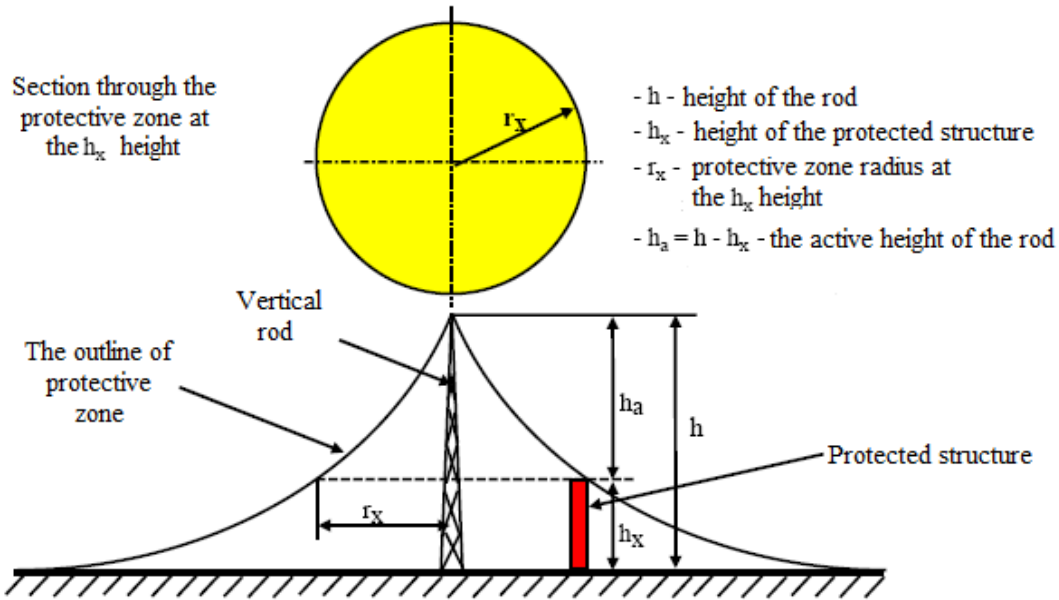


Fig.3.4. Sections through the protective zone of a vertical rod

As it can be observed from the figure presented above, the section of the protective zone at the  $h_x$  height has the shape of a circle, the radius being given by the following relation:

$$r_x = \frac{1,6 \cdot (h - h_x)}{1 + \frac{h_x}{h}} \cdot p \quad (3.3)$$

Where the efficiency of the vertical rod is given by the following parameter:

$$\begin{cases} p = 1, & \text{for } h \leq 30m \\ p = \sqrt{\frac{30}{h}} \approx \frac{5,5}{\sqrt{h}}, & \text{for } h > 30m \end{cases} \quad (3.4)$$

In order to determine the protective zone given by two vertical rods, the protective zone of a single rod must be considered, as in the outside range of the vertical rods, the protective zone is independently generated by each rod, mutual influences existing only in the internal area between the rods, as it is represented in Figure 3.5.

The inner area of the protective zone is given in its upper side by an arc, which passes through the top of the vertical rods and a point placed at the half distance between the rods at the  $h_0$  height, and by the lines that intersects in horizontal plane, at the  $b_x$  distance from the vertical rods plan.

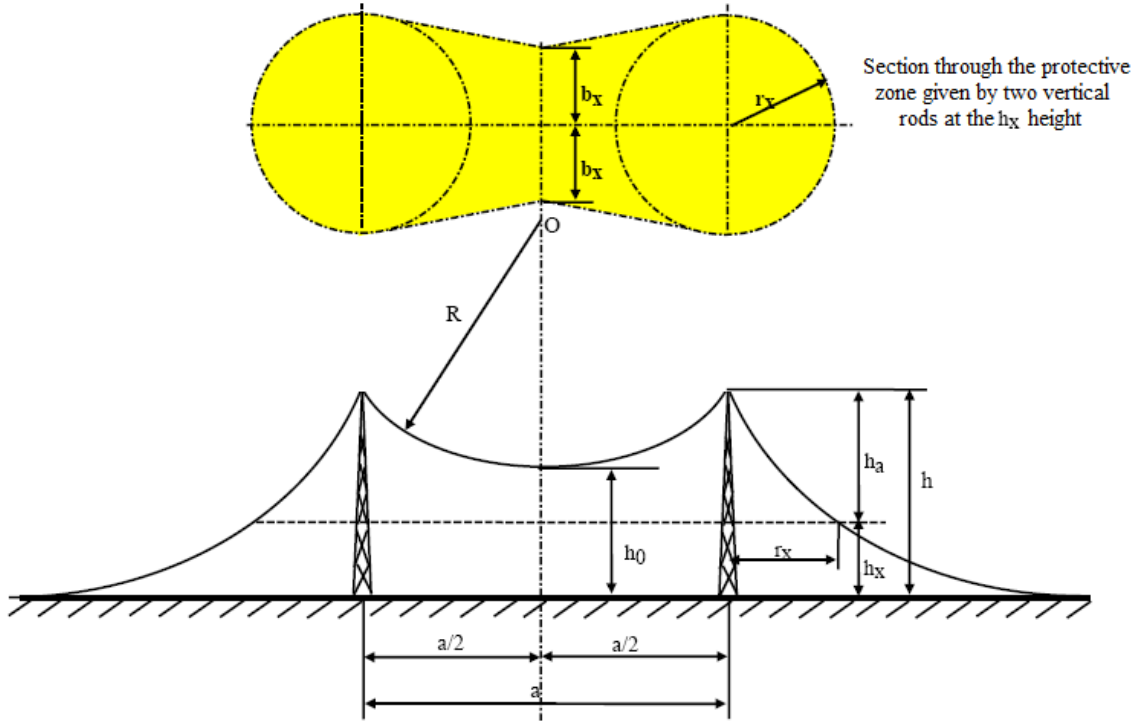


**Fig.3.5.** Protective zone generated by two vertical rods with the same height

The height of the common protective zone of the vertical rods,  $h_0$ , can be determined with the relations presented below:

$$h_0 = h - \frac{a}{7 \cdot p} \quad (3.5)$$

The specific dimension  $b_x$  of the common protective zone can be determined from normatives, and also using the following empirical relation:

$$b_x = r_x \cdot \frac{7 \cdot p \cdot h_a - a}{12.5 \cdot p \cdot h_a - a} \cdot \frac{12.5}{7} \quad (3.6)$$

The condition for which two vertical rods will have a common protective zone is that  $a < 7 \cdot h \cdot p$ .

In case of groups of three or four vertical rods, the protective zone is determined in a similar manner, as it is shown in Figure 3.6. The groups of rods presented in Figure 3.6. will have a common protective zone if the parameter  $D$ , satisfies the following condition:

$$D \leq 8 \cdot (h - h_x) \cdot p \quad (3.7)$$

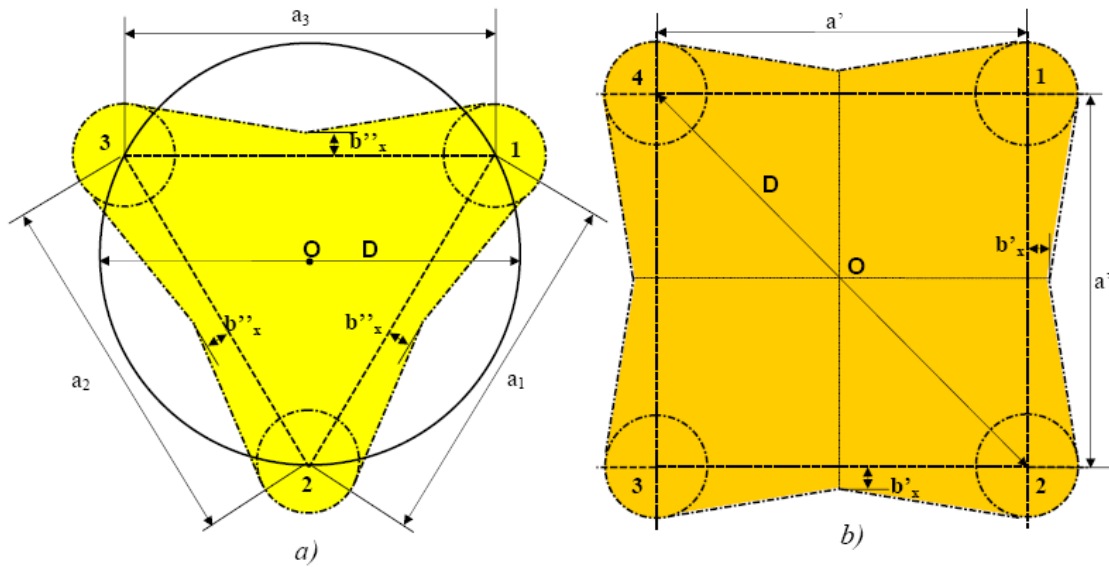


*Fig. 3.6. Protective zone generated by group of 3 or 4 vertical rods*

The same methodology is used for the case of ground wires too, as it is presented in [6].

### III.2.3. Rolling sphere method [6]

The main hypothesis of the method is based on the idea that the lightning strikes the nearest object on the earth situated at the so-called orientation distance from the descending leader's head. Thus, one can imagine one sphere which is moving towards the ground and which has the radius equal with the orientation distance. The head of the descending leader is considered to be in the center of this sphere. The first object touched by this virtual sphere will be stricken by the lightning.

The main improvement of this method is related to the fact that the orientation distance of the lightning discharge is correlated with the lightning current intensity, and not only with the height of the grounded structure, as the laboratory models method presumes. This correlation is fully acceptable because it has a real physical explanation, that is consistent with protection of the electrical installations, where a lightning with a certain current intensity generates overvoltage of a certain level.

In order to determine the orientation distance of the lightning discharge (the rolling sphere radius), several relations were developed and customized by different researchers over the time. One of the most used relation is presented below:

$$R = d = 9,4 \cdot I_t^{\frac{2}{3}} \quad (3.8)$$

where  $I_t$  represents the intensity of the lightning current.

Once the orientation distance is estimated, the protective zones generated by the lightning protection systems can be determined in a similar manner as that presented in the case of laboratory models method. The protective zone generated by a complex lightning protection system is determined for each lightning rod, or for groups of two, three, or four vertical rods, or ground wires.

For a single vertical rod, the protected area is generated by rolling the fictional sphere on the ground without losing the contact with the vertical rod, as it is presented below:

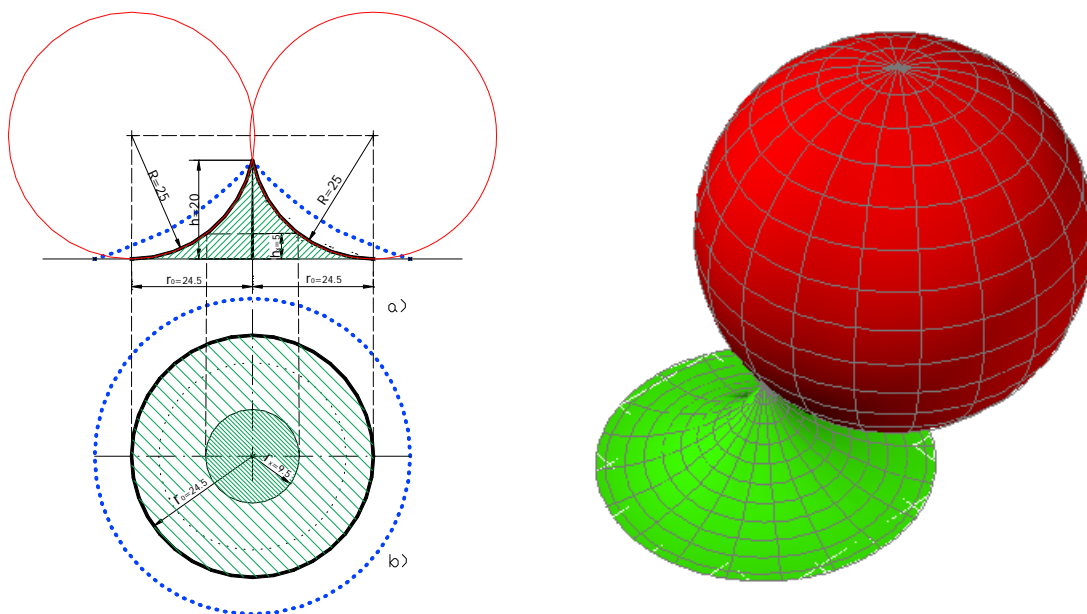


**Fig.3.7.** The protective zone of a single vertical rod: in the left side – section in the lightning rod plane (a); horizontal section at ground level and  $h_x$  height (b); in the right: a 3D representation of the protective zone generated by the rolling sphere

With blue line are represented sections through the protective area generated by the same vertical rod, when the laboratory models method was considered.

Regarding the graphical construction presented in the Figure 3.7.a and b, the following observation must be made:

- The outline of the horizontal section through horizontal planes is determined by arcs with followings radii at the ground level and at the  $h_x$  height:

$$\text{for } h < R : r_0 = \sqrt{h(2R-h)} ; r_x = r_0 - \sqrt{h_x(2R-h_x)} \quad (3.9)$$

$$\text{for } h > R : r_0 = R ; r_x = R - \sqrt{h_x(2R-h_x)} \quad (3.10)$$

Where:

- $r_0$  – horizontal section radius of the protective zone at the ground level;
- $r_x$  – horizontal section radius of the protective zone at the  $h_x$  height;
- $h_x$  – height of the protected structure;
- $h$  – height of the vertical rod;
- $R$  – rolling sphere radius.

If two adjacent vertical rods are considered, the protective zone has two components. Thus in the outside range of the vertical rods, the protective zone is independently generated by each rod, and in the inner area between the rods, the protective zone is determined by the rolling sphere, which simultaneously touches both vertical rods, without losing contact with the ground. A three dimensional representation of such graphical construction is presented below:

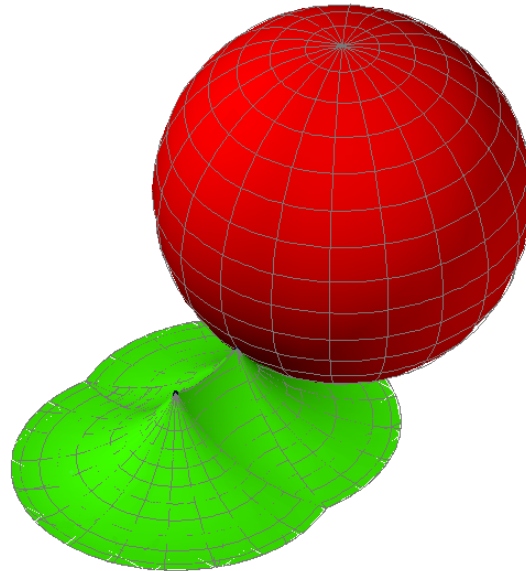


**Fig.3.8.** The protective zone of two vertical rods, given for a certain value of the lightning current

More graphical details of the dimensions of the protective zone are given in Figure 3.9., where horizontal and vertical sections through the protective zone are presented. The outline of the areas between the lightning rods, situated in vertical plane, results contacting the rolling sphere simultaneously with both lightning rods. This outline is delimited, in its superior part, by arcs whose  $R_1$  radius can be calculate with the following relations:

$$\text{for } h < R : R_1 = \sqrt{(R - h)^2 + a^2} \quad (3.11)$$

$$\text{for } h > R : R_1 = a \quad (3.12)$$

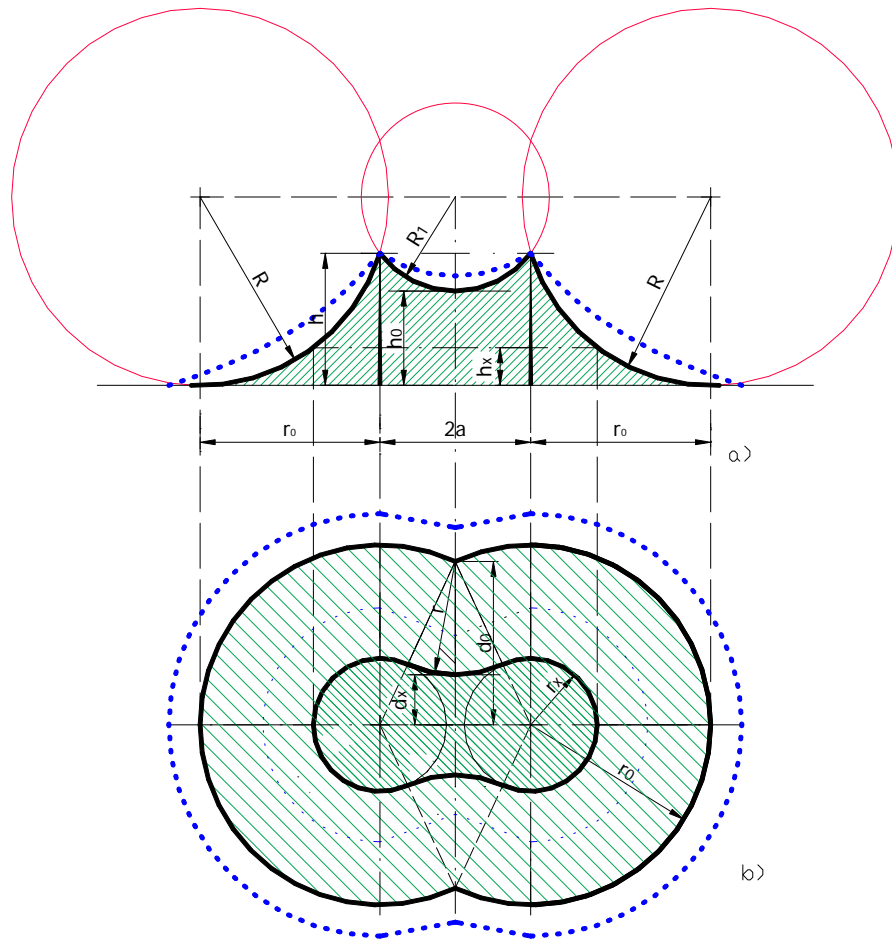


**Fig.3.9.** Vertical and horizontal sections through the protective zone of two vertical rods with the same height, when  $h < R$

These arc determines the minimum height of the protective zone, in the area between the rods, which can be calculated with the following formula:

$$h_0 = R - R_1 \quad (3.13)$$

The condition for which two vertical rods will have a common protective zone is that  $h_0 > 0$ , and thus  $R > R_1$ . This condition becomes  $a < r_0$  for  $h < R$ , and  $a < R$  for  $h > R$ . The  $r_0$  arcs intersect at the middle of distance between the rods ( $2a$ ), determining the minimal half-width of the protective zone at this level, as:

$$\text{for } h < R: d_0 = \sqrt{r_0^2 - a^2} \quad (3.14)$$

$$\text{for } h > R: r_0 = R \quad (3.15)$$

At the  $h_x$  height of the protected object, this half-width is given by the following relation:

$$d_x = d_0 - \sqrt{h_x(2R - h_x)} \quad (3.16)$$

For groups of three or four vertical rods, the outline of the protective zone is given considering two by two adjacent rods, and in the upper side, the protective zone is determined by the rolling sphere which simultaneous stands up on the rods' tips. Such graphical construction are presented below:

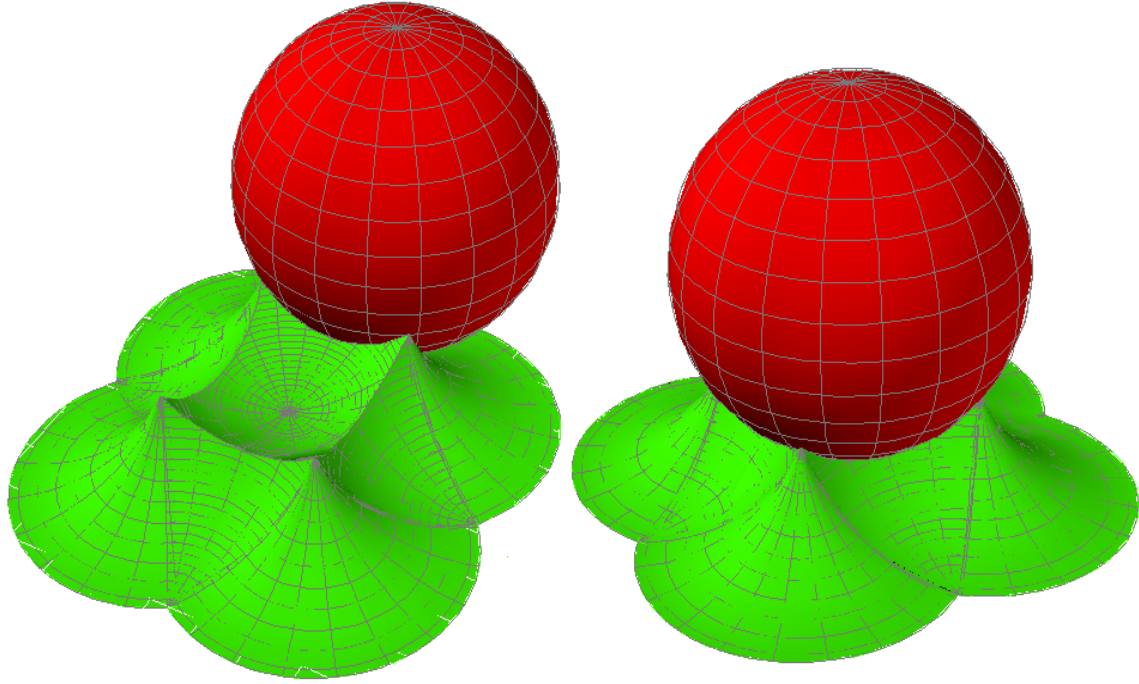


*Fig.3.10. Three dimensional representation of the protective zone of four vertical rods*

The minimum height of the protective zone between the rods can be determined with the relation presented below:

$$h_0 = h - R + \sqrt{R^2 - R_0^2} \quad (3.17)$$

where  $R_0$  is given by the following relations:

- for three vertical rods:

$$R_0 = \frac{2a_1a_2a_3}{\sqrt{(a_1 + a_2 + a_3)(a_1 + a_2 - a_3)(a_1 - a_2 + a_3)(-a_1 + a_2 + a_3)}} \quad (3.18)$$

- in case of four vertical rods:

$$R_0 = \sqrt{a_1^2 + a_2^2} \quad (3.19)$$

Where  $a_1$ ,  $a_2$  and  $a_3$  are the distances between the vertical rods ( $a_1$  and  $a_2$  for the case of four rods disposed in a rectangle, and  $a_1$ ,  $a_2$  and  $a_3$  when 3 vertical rods are disposed in a triangle).

For the case of vertical rods with different heights or for ground wires, the protective zones can be determined in a similar graphical manner, only the dimensions will be calculated with different relations, fully described in [6].

Considering all these aspects presented above it is obviously that, for a more accurate determination of the protective zones, the lightning current intensity should be precisely estimated.

### III.3. Lightning overvoltages on overhead power transmission lines

Lightning overvoltage on power transmission lines occurs due to direct lightning strokes on the component elements of the lines, or by induction in case of strokes in the line's vicinity. When lightning strikes the active conductor of the line, at the impact point current and voltage waves are formed, which propagate along the line in both directions. In the presence of the voltage wave, the potential between the active conductor and towers' components can cause the flashover of the line's insulators, from the active conductor to the line's tower. When the line's towers or the ground wires of the lines are struck, the lightning current which flows through the towers' impedance causes a voltage drop which can lead to insulators' flashover, this time from tower to the active conductor. This process is known as *backflash*. [9]

If lightning strikes in the line's vicinity then induced surges can appear on the active conductor of the line, due to electric or electromagnetic field variations, which can lead also to insulators' flashover.

Through the pulse channel of the flashover developed across the line's insulators, an electric arc discharge can be initiated, sustained by the line's operational voltage, through which a shortcircuit current is closed to ground. Thus, as a direct consequence of the lightning strikes, the overhead power line can be disconnected due to the relay protection action against the shortcircuit current.

There are two approaches of overhead lines' behavior at lightning strokes [10]:

- Some analytical models determine the pulse voltages' time evolution, considering the repeated reflections, even at the towers' level. The stress of the lines' insulators is analyzed on the basis of parameters like: towers' surge impedance, pulse surge impedance of the grounding grid, the electrostatic and electromagnetic induced voltages, the modification of the coupling factors in the presence of the corona discharge, the polarity of the pulse and the line's span.

- Others analytical models assess, only in a quantitative way, the lines' performance at lightning overvoltages on basis on specific number of outages indicator. These often used models in estimation calculations operate with the voltages' and currents' peak values, having no interest for their time evolution.

Of main concern is the specific number of outages indicator, which represents the number of line's disconnection due to direct lightning strokes across 100 km of line, over a year. The methodology generally used to determine this important indicator is presented below.

### III.3.1. Computing relation of the specific number of outages

The specific number of outages of a overhead power transmission line may have two components, one related to the direct lightning strokes in the constructive elements of the line, and other determined by the induced overvoltages in the active conductors. [6]

In order to calculate the component related to the direct lightning strokes, the number of lightning discharges which strike the analyzed power line must be initially determined. In this sense the following relation can be used:

$$N_l = D_l \cdot A_c \text{ lightnings / year} \quad (3.20)$$

where  $D_l$  is the lightning density measured in lightnings/km<sup>2</sup>·year, and the  $A_c$  represents the collection area of the lightning strokes, in km<sup>2</sup>.

The lightning density is highly related to the intensity of the weather events in the area crossed by the power line, the most common relations used to determine this parameter being presented below:

$$D_l = \frac{1,1 \cdot N_d}{1 + 1,4\sqrt{N_d}} \text{ lightnings / km}^2 \cdot \text{year} \quad (3.21)$$

where  $N_d$  is the keraunic index of the geographic area considered, given as the number of thunderstorm days over a year.

The collection area of the lightning discharges can be determined with the following relation:

$$A_c = 6 \cdot h \cdot l \text{ km}^2 \quad (3.22)$$

where  $l$  is the length of the line, in km, and  $h$  is the average height of the most exposed conductors.

Not all the lightning strokes determine the insulators' flashover, and thus the total number of flashover is determined with the relation presented below:

$$N_f = 6h \cdot l \cdot D_l \cdot P_f \text{ flashovers / year} \quad (3.23)$$

where  $P_f$  represents the impulse voltage flashover probability of the line's insulation, and it can be considered equal with probability of occurrence of a lightning current higher than the specific protective current. Considering the fact that the probability of occurrence for a lightning current having the amplitude  $I_l$  is given by an exponential law, the flashover probability can be determined with a relation having the following form:

$$P_f = P(I_l \geq I_{pr}) = A \cdot e^{-\frac{I_{pr}}{B}} \quad (3.24)$$

where parameters A and B are related to the discharge type, and are presented in the following table.

**Table 3.2.** Values of the parameters A and B from relation (3.24)

Discharge type	A [u.r.]	B [kA <sup>-1</sup> ]
Unique negative strokes or first discharge of multiple strokes	1,51	26
The following components of a negative multiple stroke	1,32	15
Positive strokes	1,00	87
Any type of strokes	1,11	35

$I_{pr}$  is the protective current of the line, which represents the minimum value of the lightning current which generates on the analyzed power line an overvoltage large enough to determine the insulators' flashover. The standardized values of the protective current are generally oversized, thus individual values for each type of line must be determined.

Even so, not all insulators' flashovers can lead to line's disconnection, but only those which turns in electric arc at industrial frequency. Thus the line's total number of disconnection can be determined with the following relation:

$$N_d = 6 \cdot h \cdot l \cdot D_l \cdot P_f \cdot P_a \text{ disconnections / year} \quad (3.25)$$

and the specific number of disconnection, for 100 km of the same type of power line, is given by the relation presented below:

$$n_d = 0,6 \cdot h \cdot D_l \cdot P_f \cdot P_a \text{ disconnections / 100 km} \cdot \text{year} \quad (3.26)$$

The  $P_a$  parameter from the last two relations is the insulators' flashover probability to develop into an electric arc. This probability can be determined with the next relation:

$$P_a = 1,6 \cdot \frac{U_s}{100 \cdot I_{ins}} - 0,06 \quad (3.27)$$

Where:

$U_s$  – is the effective value of the voltage at industrial frequency applied to the insulator which leads to line's disconnection;

$l_{ins}$  – length of the insulator, whose flashover leads to line's disconnection.

If the neutral point of the analyzed grid is effectively grounded,  $U_s$  represents the phase voltage and  $l_{ins}$  is equal with the length of a insulators' chain. For grids with isolated neutral point, or treated with compensation coil,  $U_s$  represents the line voltage and  $l_{ins}$  is considered twice as the length of a insulators' chain, because the analyzed power line will be disconnected only a double phase to ground shortcircuit will occur.

### III.3.2. The behavior of power lines without ground wires at direct lightning strokes

If ground wires are not installed on power lines, the specific number of outages of the line can be computed with the following relation:[6]

$$n_d = n_{dac} + n_{dtw} \quad (3.28)$$

where those two terms of the relation refer to the lightning strokes in active conductors and line's towers. In terms of statistical distribution of lightning strokes on such lines, 47% of all lightning discharges strike the phase conductors, and the rest of 53% strike in line's towers. Thus relation (3.28) becomes:

$$n_d = 0,47 \cdot 0,6 \cdot h_{ac} \cdot D_l \cdot P_{acf} \cdot P_a + 0,53 \cdot 0,6 \cdot h_{tw} \cdot D_f \cdot P_{twf} \cdot P_a \quad (3.29)$$

where:

$h_{ac}$  – the average height of suspension of the most exposed active conductors;

$h_{tw}$  – height of the line's towers;

$P_{acf}$  – insulation flashover probability when active conductors are stroked by lightning;

$P_{twf}$  – insulation flashover probability when line's towers are stroked by lightning.

The overhead lines which usually don't have ground wires installed are the medium voltage lines. The neutral point of such grids can be treated either with compensation coils or with resistors. Thus following situations can be considered:

#### a) *A power line of a grid with grounded neutral*

In this situation the line's disconnection is determined by the insulator's flashover from a single phase, thus the value of the protective current of the line can be calculated with the following relation:

$$I_{prac} = \frac{U_{50\%}}{Z_{kc}} \text{ kA} , \quad Z_{kc} = \frac{Z_k \cdot \frac{Z_{ac}}{2}}{Z_k + \frac{Z_{ac}}{2}} \Omega \quad (3.30)$$

where:

$U_{50\%}$  – is the flashover voltage of the line's insulator, in kV;

$Z_k$  – the characteristic impedance of the lightning discharge channel;

$Z_{ac}$  – the characteristic impedance of the active conductor to be stroked by lightning.

When line's towers are hit by the lightning, the protective value of the current can be determined with the relation presented below:

$$I_{prtw} = \frac{U_{50\%}}{\kappa \cdot R_p + \kappa^2 \cdot \frac{L_{tw}}{t_f}} \text{ kA} , \quad \kappa = \frac{Z_k}{Z_k + R_p} \Omega \quad (3.31)$$

where:

$R_p$  – pulse resistance of the lines' tower ground electrode;

$L_{tw}$  – the average inductivity of the tower, in H;

$t_f$  – front duration of the lightning voltage wave.

For the medium voltage lines, the tower impedance can be neglected in comparison with its ground electrode resistances, thus the relation presented above turns in:

$$I_{prtw} = \frac{U_{50\%}}{R_p} \text{ kA} \quad (3.32)$$

### ***b) A power line of a grid with isolated neutral or treated with compensation coil***

Such power lines will be disconnected only when double phase to ground shortcircuit occurs. When a lightning discharge strike the phase conductor, the voltage drop along the line's tower is equal with the voltage of the stroked conductor, as the following relation can be written:

$$U_{tw} = R_p \cdot I_l = U_{ac1} \quad (3.33)$$

Through the electrostatic induction, the voltage across another phase conductor is:

$$U_{ac2} = k_{ac} \cdot U_{ac1} \quad (3.34)$$

where  $k_{ac}$  is the capacitive coupling factor between those two active conductors. In this way, the voltage across this phase' insulation can be determined with the following relation:

$$U_{ins} = U_{tw} - U_{ac2} = (1 - k_{ac}) \cdot R_p \cdot I_t \quad (3.35)$$

and the protective current, when active conductors are stroked by the lightning, can be determined as:

$$I_{prac} = \frac{U_{50\%}}{(1 - k_{ac}) \cdot R_p} \text{ kA} \quad (3.36)$$

If the line's tower is stroked, then the voltage of all phases insulation is the same, and multiple shortcircuits can occur. Thus the protective current can be estimated using the following relation:

$$I_{prtw} = \frac{U_{50\%}}{R_p} \text{ kA} \quad (3.37)$$

If towers' inductance can not be neglected, then  $R_p$  from the last two relations must be replaced with the denominator expression from relation (3.31).

As all values of the protective currents can now be determined, also the associated flashover probabilities  $P_{acf}$  and  $P_{twf}$  can be estimated, according to relation (3.24).

### III.3.3. The behavior of power lines with ground wires at direct lightning strokes

The relation used to determine the specific number of outages contains in this situation three terms, associated to direct lightning strokes in phase conductors, line's towers and ground wires, as it is presented below: [6]

$$n_d = n_{dac} + n_{dtw} + n_{dgdw} \quad (3.38)$$

Due to the presence of the ground wires, only a small percentage of the lightning discharges will strike the phase conductors. The probability that the lightning discharges will pass through the protective screen generated by the ground wires is estimated with the following relation:

$$\lg P_\alpha = \frac{\alpha \cdot \sqrt{h_{gw}}}{90} - 4 \quad (3.39)$$

where:

$\alpha$  – power line's protective angle, usually  $20 \div 30^\circ$ ;

$h_{gw}$  – average suspension height of the ground wires.

The lightning discharge repartition between the line's towers and ground wires is given by the relation presented below:

$$\gamma = 4 \cdot \frac{h_{tw}}{l_d} \quad (3.40)$$

Where  $l_d$  the length between two adjacent towers, and  $h_{tw}$  is the maximum height of the line's towers.

Thus using relations (3.26) and (3.38), the specific number of outages for a power line with ground wires is determined with the following relation:

$$n_d = P_\alpha \left[ 0,6h_{ac}D_fP_{acf}P_a + (1-P_\alpha) \cdot \left[ \gamma 0,6h_{tw}D_fP_{twf}P_a + (1-\gamma)0,6h_{gw}D_fP_{gwf}P_a \right] \right] \quad (3.41)$$

When one of the phase conductors is stroked by the lightning discharge, the voltage's amplitude which propagates along it is determined as:

$$U_{ac} = Z_{kc} \cdot I_l \quad (3.42)$$

Where  $Z_{kc}$  is given by relation (3.30). Through electrostatic induction, this voltage wave generates a voltage wave on ground wires, and if the connection between ground wires and line's towers is considered, the voltage on the adjacent towers is given by the relation:

$$U_{gw} = k_{gw} \cdot U_{ac} = U_{tw} \quad (3.43)$$

Where  $k_{gw}$  is the capacitive coupling factor between the active conductor struck by lightning and ground wires.

The voltage on the phase insulators of the adjacent towers is:

$$U_{ins} = U_{ac} - U_{tw} = (1 - k_{gw}) \cdot Z_{kc} \cdot I_l \quad (3.44)$$

As active conductors are struck by lightning discharge, the associated protective current is determined by the following relation:

$$I_{prac} = \frac{U_{50\%}}{(1 - k_{gw}) \cdot Z_{kc}} \text{ kA} \quad (3.45)$$

Where  $Z_{kc}$  is given by relation (3.30).

If line's towers are hit by the lightning, the voltage drop which occurs can be determined as:

$$U_{tw} = \left( \kappa_1 \cdot R_p + \kappa_1^2 \cdot \frac{L_{tw}}{t_f} \right) \cdot I_l = U_{gw} \quad (3.46)$$

Due to capacitive coupling between ground wires and phase conductor, the voltage induced on the last ones, is equal with:

$$U_{ac} = k_{gwac} \cdot U_{gw} \quad (3.47)$$

Where  $k_{gwac}$  is the capacitive coupling factor between the ground wire and the most remote active conductor.

The voltage which will stress the insulation is in fact the difference between the towers' voltage and the voltage of the most remote phase conductor. If this voltage is equal with flashover voltage, the protective current is given by the following relation:

$$I_{prtw} = \frac{U_{50\%}}{(1 - k_{gwac}) \cdot \left( \kappa_1 \cdot R_p + \kappa_1^2 \cdot \frac{L_{tw}}{t_f} \right)} \text{ kA} \quad (3.48)$$

where:

$$\kappa_1 = \frac{\frac{Z_k \cdot Z_{gw} / 2}{Z_k + Z_{gw} / 2}}{\frac{Z_k \cdot Z_{gw} / 2}{Z_k + Z_{gw} / 2} + R_p} \quad (3.49)$$

where  $Z_{gw}$  is the ground wire characteristic impedance, in  $\Omega$ .

For the case of ultra high voltage power lines the insulation stress imposed by the lines' operational voltage, and the electromagnetic and electrostatic induced voltages between the lightning discharge channel and line's conductors, active or ground wire, can no longer be neglected. If all these elements are considered, then the protective current when line's towers are struck is given by the relation presented below:

$$I_{prtw} = \frac{U_{50\%} - 0,5 \cdot U_{ph}}{(1 - k_{gwac}) \cdot \left( \kappa_1 \cdot R_p + \kappa_1^2 \cdot \frac{L_{tw}}{t_f} + 0,5 \cdot \frac{h_{gw}}{t_f} \right) + \left( 1 - k_{gwac} \frac{h_{gw}}{h_{ac}} \right) \cdot \frac{h_{ac}}{t_f}} \quad (3.50)$$

where  $U_{ph}$  is the effective value of the phase voltage associated to the highest voltage of the grid, in kV, and  $t_f$  is the front time of impulse, in  $\mu$ s.

When ground wires are struck, both towers of the line's span share the current leakage to the ground, thus:

$$I_{prgw} \cong 2I_{prtw} \quad (3.51)$$

In these circumstances, the associated flashover probabilities,  $P_{acf}$ ,  $P_{twf}$  and  $P_{gwf}$ , can now be determined.

### III.3.4. The total specific number of disconnections

The total specific number of disconnections is composed of the specific number of outages related to direct strokes, and from those generated by the lightning induced overvoltages, as:

$$n_t = n_d + n_{io} \quad (3.52)$$

The specific number of flashovers related to induced overvoltages can be determined as following:

$$n_{f,io} = \frac{6 \cdot A \cdot B \cdot D_l \cdot h}{U_{50\%}} \cdot e^{-\frac{U_{50\%LEA}}{10 \cdot B}} \quad (3.53)$$

Where notations have the same significance as in § III.3.1. , except  $h$  which represent the average suspension height of the conductor disposed at the highest altitude.

Thus specific number of disconnections is:

$$n_{io} = n_{f,io} \cdot P_a \quad (3.54)$$

where  $P_a$  is given by (3.27).

If relations (3.28) or (3.38), depending on the presence or the absence of the ground wire, and (3.54) are replaced in (3.52) the total specific number of outages for the analyzed power line is obtained.

### III.4. Lightning overvoltages in power stations

The complex installations of power stations must be protected against direct lightning strokes, but also against surge waves coming from power lines. While the protection against direct lightning strokes is ensured through a protective system with vertical rods or ground wire, the protection against the overvoltage waves coming from power lines is achieved with variable resistance surge arresters.[6]

Lightning overvoltage analysis in power stations aims selection and proper installation of surge arresters. It is also necessary to verify if the power stations' devices are in the protective area of the existing surge arresters.

The level of lightning overvoltages in power stations can be determined in two manners: [6]

- A comprehensive analysis of the surge waves' propagation process, considering its multiple reflections and refractions in different points of the station;
- The transient regime analysis, generated by the lightning surge waves, which excites the power station's complex circuits, using the laws of electrical circuits.

The second approach is practically useless without some adequate software applications support. First method is also very complex, if an un-simplified scheme of the power station is used. Even so, after many studies on physical models it seems that it is possible to simplify the power stations' equivalent scheme, redistributing the equipment's surge capacities. In this sense, the so called moment rule is applied, redistributing the equipments' capacities in the main points of the scheme, depending on the distance between the concentration node and the point where capacity was in the first scheme.

Usually the surge capacities of the equipments are concentrated in the points where transformers and surge arresters are installed in the power station. The oversimplification of the power stations' scheme involves inherently larger calculation errors, as a single propagating path is considered, with only one surge arrester connected, and a single concentrated capacity. In this situation all capacities are concentrated in transformers' point. Depending on the relative position of those two circuit elements, and the propagating path of the incident wave, the following situation can be considered: [6]

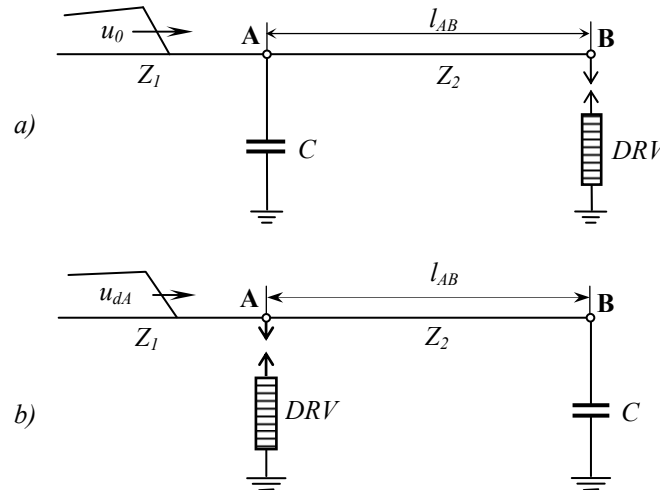


**Fig.4.1.** Simplified equivalent diagrams used for lightning overvoltages determination in power stations: a) diagram with upstream capacity; b) diagram with upstream surge arrester, related to wave propagation direction.

where:

$C$  – power stations' equivalent surge capacity;

$DRV$  – surge arrester with variable resistance;

$Z_1$  – power lines' characteristic impedance;

$Z_2$  – power station's busbars characteristic impedance;

$l_{AB}$  – distance between the considered points (usually represents the actual distance between the surge arrester and power transformer, or the maximum distance between such types of equipments from a power station);

$u_0, u_{dA}$  – incident voltage waves (direct wave in point A).

For such simple schemes, the level of the overvoltage which stresses the transformers' insulation can be estimated with different graphical and analytical methods.

For the case considered in Fig.4.1.a, the presence of capacity is neglected in the first stage. Thus a new simplifying hypothesis is considered, but the analysis results are good enough, as the effect of the capacity presence is to reduce the surge wave slope. Applying the Petersen rule on this new propagating scheme, the equivalent lumped parameters scheme is obtained, as it is presented in Figure 4.2. This equivalent scheme can be

considered only when the lines' and bus bars' characteristic impedances are equal ( $Z_1 = Z_2 = Z$ ). The current will flow through the circuit only while the surge arrester is operational.

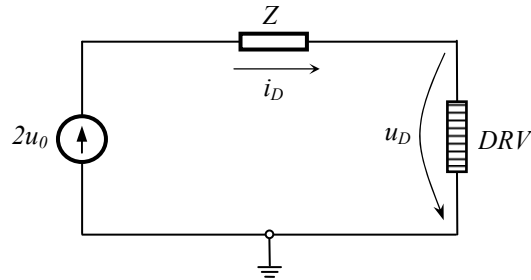


**Fig.4.2.** Equivalent scheme resulted by applying Petersen's rule and neglecting the capacity for the diagram presented in Fig.4.1.a

The following equations describe the circuit presented above, after the surge arrester becomes operational:

$$\begin{cases} 2 \cdot u_0 = Z \cdot i_D + u_D \\ u_D = f(i_D) \end{cases} \quad (4.1)$$

Where the second equation is the voltage-current characteristic of surge arrester's nonlinear resistor.

Because of the nonlinear character of the voltage-current characteristic of surge arrester's resistor, the equations' system (4.1) must be solved using the characteristics method (Bergeron's method). The left term of the first equation is represented like a typical function, in the first quadrant of the axis system –  $u_0t$ . The second equation and the right term of the first one, are represented as a function of the surge arrester's current intensity, in the second quadrant of the axis system –  $u_0i_D$ . Until the surge arrester becomes operational, the variation of its voltage is given by the incident wave ( $2u_0$ ). After that, the voltage variation across the surge arrester is determined as following:

- for different voltage levels absciss parallel lines will be drawn;
- at the intersection point of these lines with the curve describing first equation's terms, line segments will be drawn parallel with the ordinate;
- at the intersection of the segments drawn in quadrant II, with the  $u_D = f(i_D)$  characteristic, a new segment is drawn, parallel with the absciss;
- the surge arrester's voltage level is obtained at the intersection of the last segment with the vertical segment drawn in quadrant I, at the specific moment in time.

The graphical representation of the characteristic methods is given the figure below, where the  $u_D = f(i_D)$  characteristic can be observed in the first quadrant:[6]

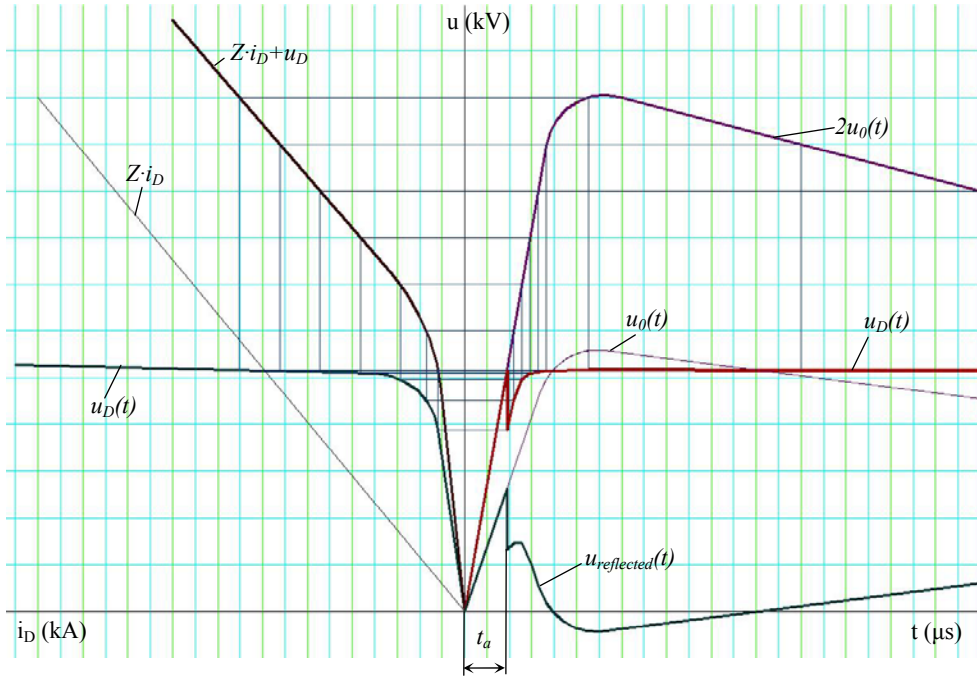


**Fig. 4.3.** An example of characteristics method implementation model for the equations' system (4.1)

The voltage in point **A** is determined considering the voltage of the incident wave ( $u_0$ ) and the amplitude of the wave reflected from point **B**, at the same time. In order to estimate the reflected wave's time evolution –  $u_{reflected}(t)$  – it must be considered that for any point of the grid in any moment, that the voltage is represented by the sum of the incident voltage wave and the reflected one, as presented below:

$$u_D = u_0 + u_{reflected} \Rightarrow u_{reflected} = u_{B \rightarrow A} = u_D - u_0 \quad (4.2)$$

This equation can be solved in a graphical manner, as it is presented in Figure 4.3.

When the incident wave and the reflected one are added in point **A**, it must be considered that the reflected wave from point **B** propagates along the bus bars section, having the length  $l_{AB}$ , in a certain period of time. Thus if the moment when the incident wave arrives in point **A** is considered the first moment of the analysis, then the reflected wave arrive in in point **A** after a period of time  $\tau$ , determined as following:

$$\tau = \frac{2 \cdot l_{AB}}{v} \quad (4.3)$$

In a graphical approach this phenomenon is represented in the figure below:

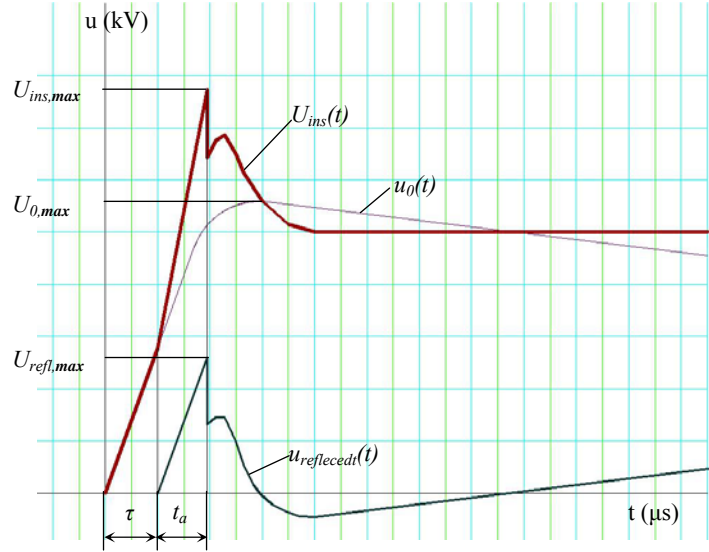


**Fig.4.4.** Graphical representation of the adding process of the incident and reflected wave in the capacitive node of the propagation scheme from Fig.4.1.a.

Thus the voltage which will stress the insulation of the equipment connected in point **A** is determined by solving the following system of equations:

$$\begin{cases} u_A(t) = u_{ins}(t) = u_0(t) + u_{reflected}(t - \tau) \\ \tau = \frac{2 \cdot l_{AB}}{v} \end{cases} \quad (4.4)$$

Where  $v$  is the propagation speed of the electromagnetic waves on power station's bus bars, which usually is considered equal with the speed of light.

From Figure 4.3. it can be observed that until  $t_a$  moment, when the surge arrester becomes operational, the reflected wave's slope is equal with the incident wave's slope from point **A**. Thus from Figure 4.4., the maximum level of the voltage which stresses the equipments' insulation from point **A**, is given by the following expression:

$$U_{ins,max} = u_0(t_a + \tau) + u_{reflected}(t_a) = a \cdot (t_a + \tau) + a \cdot t_a = U_{res} + \frac{2 \cdot a \cdot l_{AB}}{v} \quad (4.5)$$

Where  $a$  is the front slope of the voltage wave, and  $U_{res}$  is the residual voltage at surge arrester's nominal current, which is equal with its flashover voltage.

Once a relation as (4.5) is obtained, it can be used to test de protection given by the surge arresters, without drawing the graphical constructions such as those presented in Figure 4.3. and 4.4.

For the case of Figure 4.1.b, where the capacity is connected after the surge arrester, in the wave's propagation sense, at the beginning the presence of capacity is neglected. Thus the time variation of the surge arrester's voltage is determined, neglecting also the presence of the reflected wave, as the bus bars section having the characteristic impedance  $Z_2$  is considered as infinitely long. Applying Petersen's rule on this new propagation scheme, the following equivalent diagram with lumped parameters is obtained:

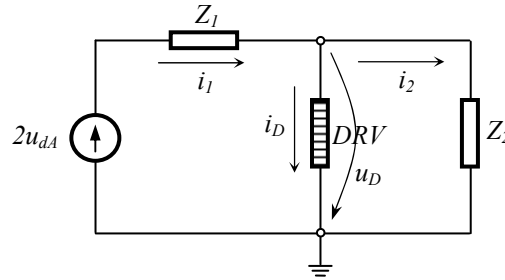


**Fig.4.5.** Equivalent diagram obtained using Petersen's rule for the diagram presented in Fig.4.1.b, when concentrated capacity and reflections from the bus bars' end are neglected

The following equations describe the circuit presented above, after the surge arrester becomes operational:

$$\begin{cases} 2 \cdot u_{dA} = Z_1 \cdot i_1 + u_D \\ i_1 = i_D + i_2 \\ i_2 = \frac{u_D}{Z_2} \\ u_D = f(i_D) \end{cases} \quad (4.6)$$

Where the last equation describes the current-voltage characteristic of the surge arrester's non linear resistor. If the characteristic impedances of the line and bus bars are considered equal ( $Z_1 = Z_2 = Z$ ), system (4.6) becomes:

$$\begin{cases} u_{dA} = \frac{Z}{2} \cdot i_D + u_D \\ u_D = f(i_D) \end{cases} \quad (4.7)$$

This last system of equations can be used in a similar manner, as system (4.1), using the characteristic method, but for another value of the incident wave in surge arrester's connection node, and for other parameter of the first term from first equation's right member. The graphical representation of the method applied for this system of equations is given in Figure 4.6.

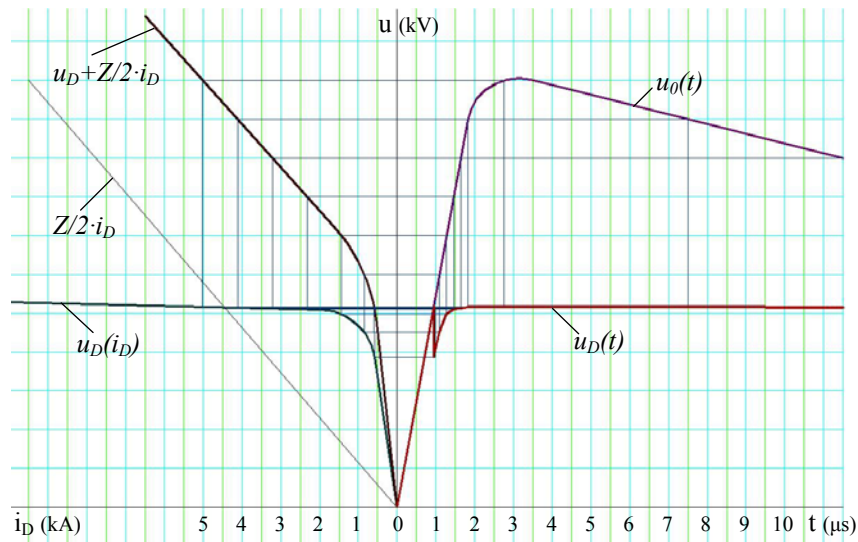


**Fig.4.6.** An example of characteristics method implementation model for the equations' system (4.7)

Considering all the simplifying hypothesis presented by now, the surge arrester's voltage time evolution,  $u_D = f(t)$ , is obtained in the first quadrant of the coordinating axis system. This voltage wave given by the surge arrester, becomes an incident wave for the surge equivalent capacity, as presented in the propagation diagram from Figure.4.7.a. The associated equivalent scheme, obtained with the Petersen's rule, is also presented in Figure.4.7.b: [6]

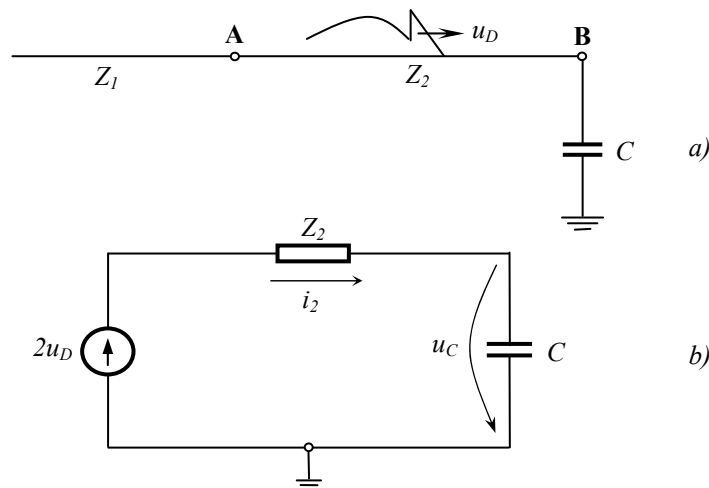


**Fig.4.7.** Propagation diagram used to determine the insulation's voltage (a) and its equivalent scheme obtained with Petersen's rule (b)

For the equivalent diagram presented in Figure 4.7.b, the following system of equations can be written:

$$\begin{cases} 2 \cdot u_D = Z_2 \cdot i_2 + u_C \\ i_2 = C \cdot \frac{du_C}{dt} \end{cases} \quad (4.8)$$

While the time variation law of the voltage in the capacitive node,  $u_C(t)$ , can be determined by solving the following differential equation:

$$\frac{du_C}{dt} + \frac{1}{T} \cdot u_C = \frac{2 \cdot u_D}{T} \quad (4.9)$$

Where  $T$  is the circuit time constant,  $T = Z_2 \cdot C$ .

Lightning voltage waves are hard to describe using relative simple functions, as they are affected by the surge arrester's flashover, multiple reflections and corona impulse discharge. As consequence, relations like (4.9) can be solved only in a combined graphical and analytical manner, using the so called sub-tangent method, as it is presented in the figure below:

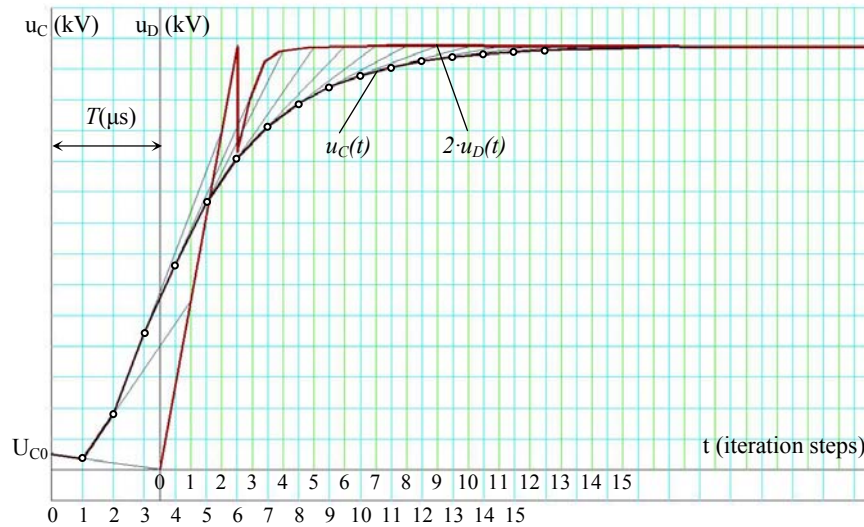


**Fig.4.8.** An example of implementation of the sub-tangent method in order to solve the differential equation (4.9)

The graphical representation from the figure above was drawn considering that the distance between points **A** and **B** ( $l_{AB}$ ) is large enough that the voltages in those two points are not influenced by the reflected wave from **B**. This hypothesis generally leads to significant errors, because in reality the distances between the surge arresters and the protected equipments are relatively small. Thus the voltage  $u_D(t)$ , as it was represented in Figure 4.7. can not be considered as an incident wave along the whole analysis time period. If the distance between the surge arrester and its protected equipment is about 100

m, the reflected wave will arrive in point **A** after  $0.67 \mu\text{s}$ , related to the moment when the incident wave reached point **A**. The voltage shape in point **A** is given exclusively by the surge arrester, but only for this time period ( $0.67 \mu\text{s}$ ), which is too short for an accurate analysis. As consequence, the voltage in **A** is obtained considering the voltage given by the surge arrester and also the reflected wave from **B**. This resulting wave becomes an incident wave for the point where equipment's insulation stress is analyzed.

The  $u_c(t)$  characteristic is determined as following: [6]

- two coordinate systems are drawn, delayed in time with  $T$  constant;
- the same voltage and time's scale is adopted for both the axis systems;
- an initial value of the voltage on capacity is adopted (such as the peak value of the alternative voltage at industrial frequency);
- at the same moment of time, the points of both voltage curves are joined;
- at the next moment in time in the axis system  $u_c0t$ , a line segment is drawn parallel with y-axis;
- the  $u_c$  voltage in the current step is obtained at the intersection point of this line segment with the previously drawn segment, between the values  $u_c$  and  $2u_D$ ;
- the same principle is used until the maximum value of the  $u_c$  voltage is obtained; usually is enough to pass the first maximum point of this function.

In order to reduce the errors an appropriate value of the time interval associated to the calculation's step have to be adopted. A larger calculation step can lead to neglect some of voltage's peaks, as it is the case with the peak voltage in the surge arrester's flashover area, presented in Figure 4.8. But this situation doesn't introduce a significant error, as this voltage peak is reduced by the corona impulse discharge. Yet a higher calculation step is not justified for all situations. The calculation step must be chosen considering the distance between those two nodal points, and the waves' propagation time on the bus bars' section. Even if the coordinate systems are not delayed with an integer number of calculations steps, is preferable that the calculation step to be determined by dividing the wave's propagation time to an integer number. The calculation step can be equal with the wave's propagation time, but it can not exceed the roundtrip propagation time for this section. [6]

## IV. Power Equipments Insulation Coordination

As IEEE and IEC specify, by insulation coordination the following aspects can be understood:

- The selection of insulation strength consistent with expected overvoltages to obtain an acceptable risk of failure (IEEE 1313.1-1996, Standard for insulation coordination).
- The selection of the dielectric strength of equipment in relation to the voltages which can appear on the system for which the equipment is intended and taking into account the service environment and the characteristics of the available protective devices (IEC 71-1, 1993, Insulation coordination).

The insulation configuration represents the complete geometric configuration of the insulation, including all elements (insulating and conducting) that influence its dielectric behavior. Examples of insulation configurations are phase-to-ground insulation, phase-to-phase insulation and longitudinal insulation [11].

For electrical equipments the following types of insulation can be considered:

### ***1. Longitudinal insulation:***

- An insulation configuration between terminals belonging to the same phase, but which are temporarily separated into two independently energized parts (open-switch device) (IEEE).
- An overvoltage that appears between the open contact of a switch (IEC).

### ***2. External insulation:***

- The air insulation and the exposed surfaces of solid insulation of equipment, which are both subject to dielectric stresses of atmospheric and other external conditions such as contamination, humidity, vermin, etc. (IEEE).
- The distances in atmospheric air, and the surfaces in contact with atmospheric air of solid insulation of the equipment which are subject to dielectric stresses and to the effects of atmospheric and other external conditions, such as pollution, humidity, vermin, etc. (IEC).

### ***3. Internal insulation:***

- Internal insulation comprises the internal solid, liquid, or gaseous elements of the insulation of equipment, which are protected from the effects of atmospheric and other external conditions such as contamination, humidity, and vermin (IEEE, IEC similarly).

### ***4. Self-restoring insulation:***

- Insulation that completely recovers its insulating properties after a disruptive discharge caused by the application of a test voltage; insulation of this kind is generally, but necessarily, external insulation (IEEE).

- Insulation which completely recovers its insulating properties after a disruptive discharge (IEC).

**5. Non-self-restoring insulation:**

- An insulation that loses its insulating properties or does not recover them completely after disruptive discharge caused by the application of a test voltage; insulation of this kind is generally, but not necessarily, internal insulation (IEEE).
- Insulation which loses its insulating properties, or does not recover them completely, after a disruptive discharge (IEC).

Although simple in concept, involving comparisons between maximum network overvoltages and minimum insulation breakdown voltages, in practice insulation coordination is a complex process.

Insulation strength of individual parts of the system or equipment is closely affected by the following factors of the impinging overvoltages: [11]

- Characteristics of overvoltages (magnitude, shape, duration, polarity of the applied voltages);
- Insulation design of the electric field distribution in the insulation;
- Type of insulation (gaseous, liquid, solid or a combination);
- Physical state of the insulation (temperature, pressure, mechanical stress, etc.)
- Operation and maintenance history of individual insulation materials.

The impinging overvoltages may exceed permissible insulation levels of individual parts of the system, so that these overvoltages should be reduced within permissible levels, or the insulated equipment should be safely protected against such overvoltages. This is essential to avoid insulation damage of equipment or to prevent possible undesirable system performance.

The magnitudes, the wave shapes (steepness of the voltages) and the time duration of overvoltages are important factors in regard to the stress on the insulation. Taking such important factors into account, the characteristics of overvoltages are generally classified into the following categories by authorities like the IEC and/or national standards bodies: [11]

- a) *Maximum continuous (power frequency) overvoltage*:  $U_s$  (MCOV). This can originate from the system under normal operating conditions.
- b) *Temporary overvoltage (TOV)*. This can originate from faults, switching operations such as load rejection, resonance conditions, non-linearity (ferro-resonance), or by a combination of these.
- c) *Slow-front overvoltages*. These can originate from switching operations and direct lightning strikes to the conductors of overhead lines.
- d) *Fast-front overvoltages*. These can originate from switching operations, lightning strikes or faults.

- e) *Very fast-front overvoltages*. These can originate from faults or switching operations in gas insulated switchgear (GIS).

The insulation strength or insulation withstanding voltage levels are expressed in terms of three representative categories of overvoltages, namely BIL, BSL and the highest power frequency voltages, as principal concepts of insulation coordination. [11]

The IEEE definitions of BIL and BSL are as follows:

- ✓ ***BIL (Basic Lightning Impulse Insulation Level)***: The electrical strength of insulation expressed in terms of the crest value of a standard lightning impulse under standard atmospheric conditions. BIL may be expressed as either statistical or conventional.
- ✓ ***BSL (Basic Switching Impulse Insulation Level)***: The electrical strength of insulation expressed in terms of the crest value of a standard switching impulse. BSL may be expressed as either statistical or conventional.
- ✓ ***Conventional BIL***: The crest value of a standard lightning impulse for which the insulation shall not exhibit disruptive discharge when subjected to a specific number of applications of this impulse under specified conditions, applicable specifically to non-self-restoring insulations.
- ✓ ***Conventional BSL***: The crest value of a standard switching impulse for which the insulation does not exhibit disruptive discharge when subjected to a specific number of impulses under specified conditions, applicable to non-self-restoring insulations.

In today's systems for voltages up to 245 kV the tests are still limited to lightning impulses and one-minute power frequency tests. Above 300 kV, in addition to lightning impulse and the one-minute power frequency tests, tests include the use of switching impulse voltages.

## References

- [1] *High-Voltage Engineering Theory and Practice*, M. Khalifa, Cairo University, Giza, Egypt, Published by Marcel Dekker, New York 1990;
- [2] *High Voltage Engineering Fundamentals, Second Edition*, E. Kuffel, W.S. Zaengl, J. Kuffel, Published by Newnes, an imprint of Butterworth-Heinemann, Great Britain 2000;
- [3] *Tehnica Tensiunilor Inalte – Aplicații*, Mircea Gușă, Marcel Istrate, Claudiu Bucă, Casa de Editură Venus, Iași 2006;
- [4] *Lightning Protection*, Vernon Cooray, The Institution of Engineering and Technology, London, 2010;
- [5] *Lightning: Principles, Instruments and Applications, Review of a Modern Lightning Research*, Hans Dieter Betz, Ulrich Schumann, Pierre Laroche, Springer 2009;
- [6] *Studiu privind expertizarea instalațiilor de 110 și 220 kV din statia FAI, urmare modificării schemelor de conexiuni, prin metoda electrogeometrica, privind riscul producerii loviturilor directe de trasnet in echipamentele statiei*, Marcel Istrate, Mircea Gușă, Dragoș Machidon, Marian Dragomir, Contract 9958P/2009 Beneficiar CN Transelectrica SA, Iași 2009;
- [7] *IEEE Std. 998, Guide for direct lightning stroke shielding of substations*, 1996, Reaffirmed 2002;
- [8] *IEC – 62305, Protection Against Lightning*, Ed. 1.0b, 2006;
- [9] *Tehnica Tensiunilor Înalte. Supratensiuni în Sistemele Electroenergetice*, Mircea Gușă, Nicolae Gavrițaș, Marcel Istrate, Constantin Asaftei, Editura Fundației Culturale “Renașterea Română” , Iași 1997;
- [10] *Analysis of Lightning’s Strokes on HV Lines in an ATP Approach*, Istrate M., Gusa M., Acta Electrotechnica, Proceedings of the 2<sup>nd</sup> International Conference on Modern Power Systems MPS 2008, pp 162-165, ISSN 1841-3323, 2008;
- [11] *Handbook of Power System Engineering*, Yoshihide Hase, John Wiley & Sons Ltd, Chichester, England 2007.